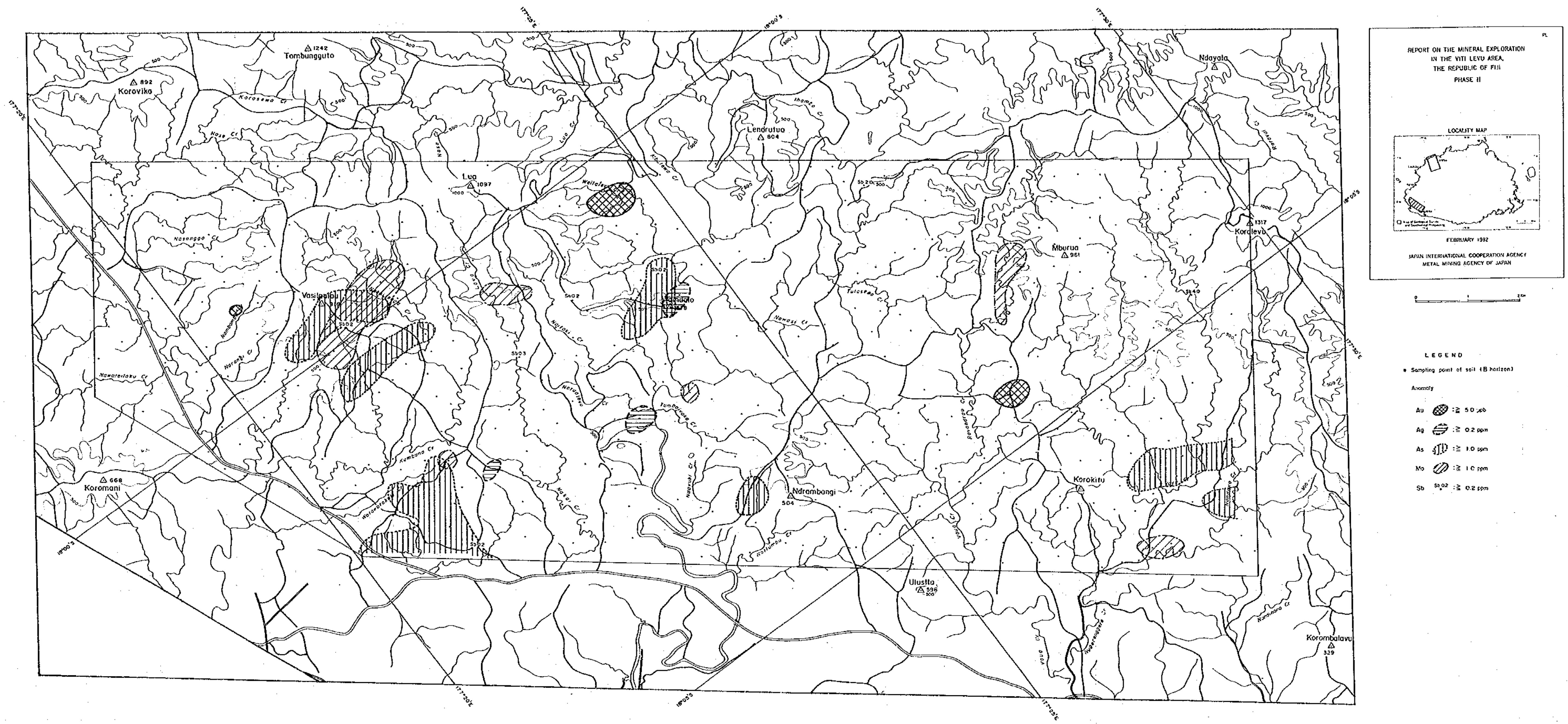

Fig. 2-3-8 Distribution of Au, Ag, As, Sb and Mo Anomalies in Soils (Sigatoka Area)

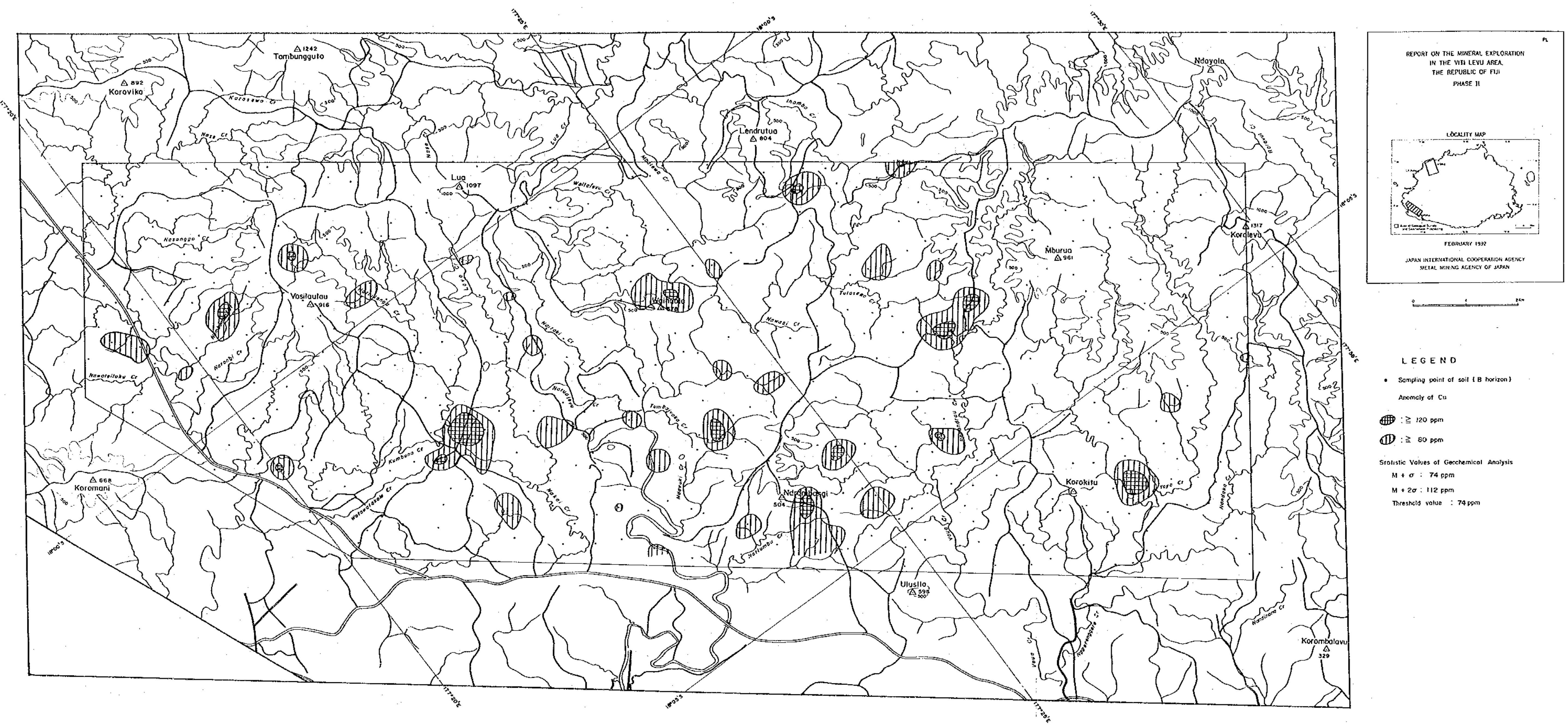

Fig. 2-3-9 Distribution of Cu Anomalies in Soils (Sigatoka Area)

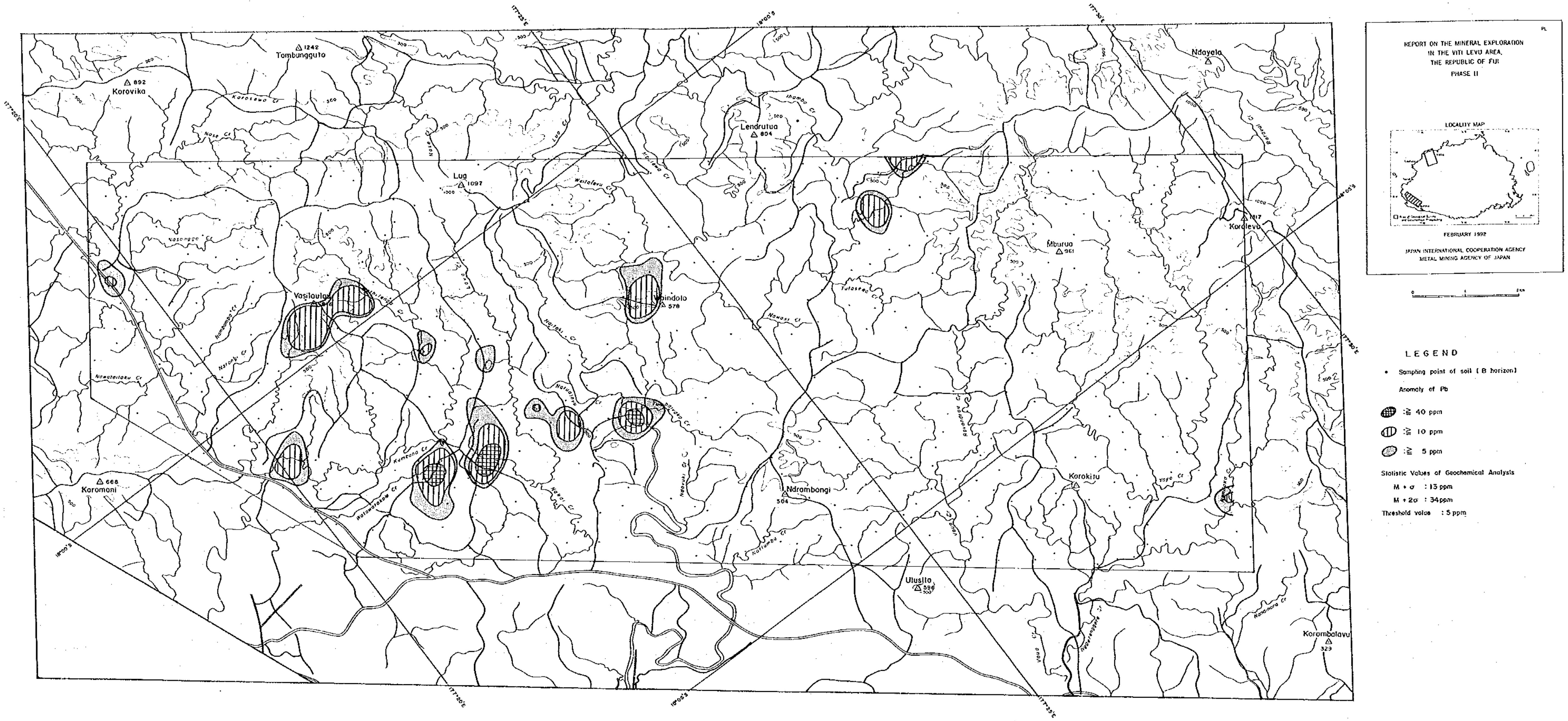

Fig. 2-3-10 Distribution of Pb Anomalies in Soils (Sigatoka Area)

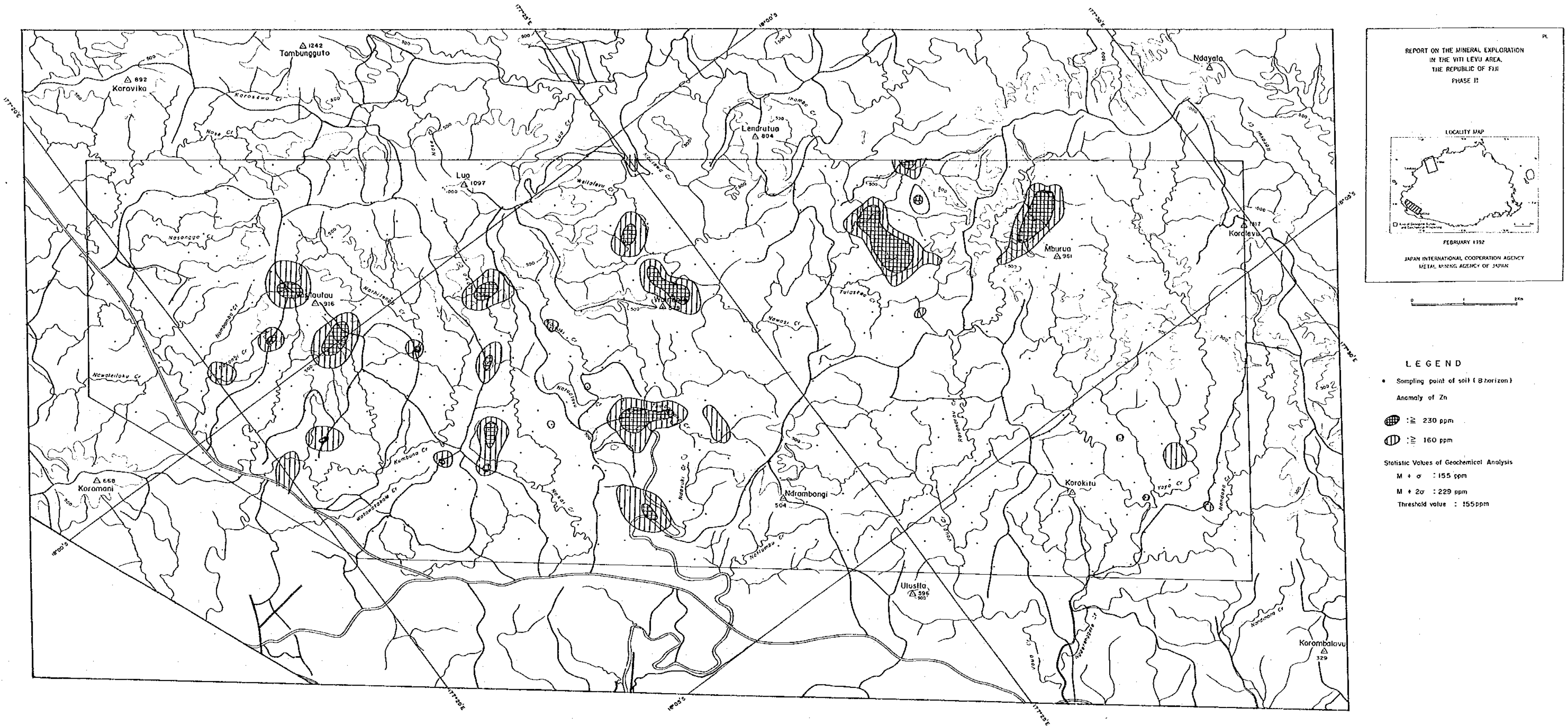

Fig. 2-3-11 Distribution of Zn Anomalies in Soils (Sigatoka Area)

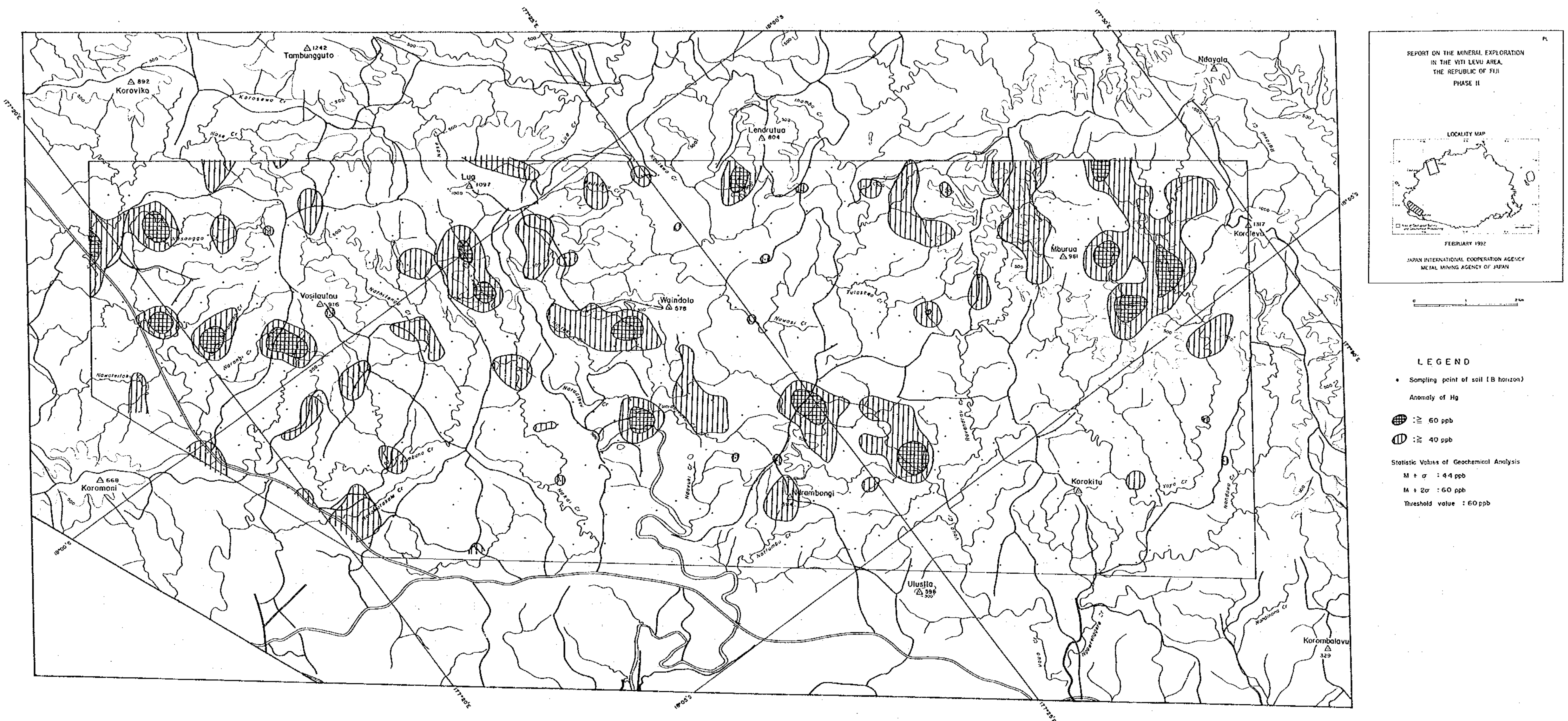

Fig. 2-3-12 Distribution of Hg Anomalies in Soils (Sigatoka Area)

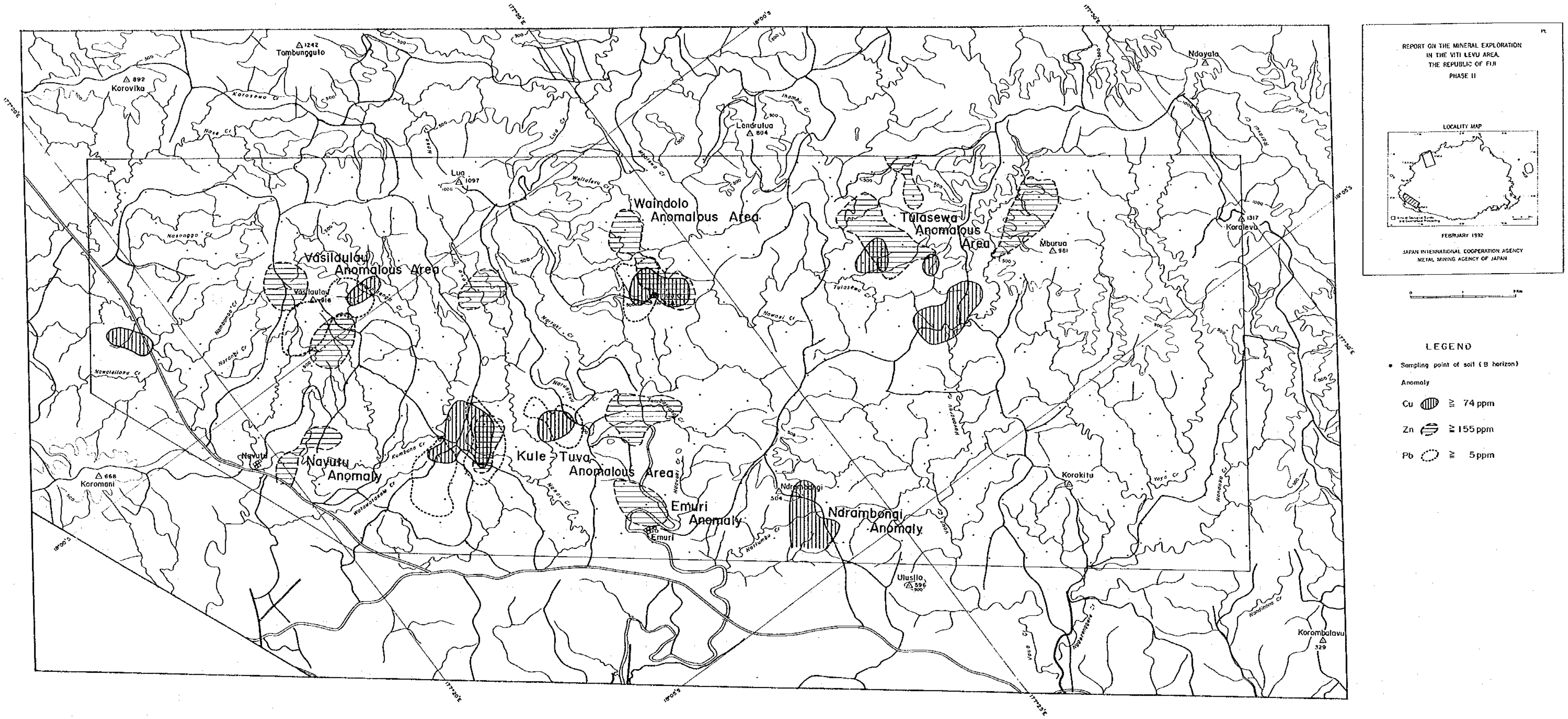

Fig. 2-3-13 Distribution of Cu, Pb and Zn Anomalies in Soils (Sigatoka Area)

This area has been prospected in the past for Cu, Pb, Zn base metals, and weak correlation is observed between Pb and Zn. Therefore, the zones with significant density of anomalies of these two elements were re-extracted as "geochemical anomalous areas" (Fig.2-3-13). During this work, parts with only one anomaly was excluded as a singular point.

For the five elements, Au, Ag, As, Sb, Mo, all points with contents exceeding the detection limit were treated as anomalies and thus these are of small significance, but those which overlap with Cu, Pb, Zn, anomalies were considered.

The following four zones were extracted as geochemically anomalous.

Tulasewa Anomalous Area

This is distributed surrounding the Tulasewa Alteration Zone. It partly overlaps with the altered zone, but most is in the unaltered parts. The anomalies are of Cu. Zn and Pb anomalies are not found.

Waindolo Anomalous Area

This zone extends to the southeast of the Waindolo Alteration Zone and partly overlaps with the most strongly altered part (Subzone I). Not only Cu, Pb, Zn, but also Ag and As anomalies overlap the Subzone I, therefore this is considered to be a noteworthy mineral showing.

Vasilaulau Anomalous Area

This zone extends from the Vasilaulau Alteration Zone to the north. It consists mainly of Pb and Zn anomalies and small Cu anomalies overlap in the eastern edge. Also there are overlapping As and Mo anomalies.

Kule-Tuva Anomalous Area

This zone extends from the Kule Alteration Zone to the Tuva Alteration Zone in the NW-SE direction. It consists of Cu, Pb, Zn anomalies.

Aside from the above, there are small independent anomalous zones at Navutu, Emuri, Lovo Creek, Ndrambongi and other localities. At Lovo Creek, Mo anomaly overlaps and scattered silicified, pyritized exposures are confirmed. But in other localities, mineralization-alteration is not confirmed.

3-4-5 Results of geochemical prospecting

Many of the geochemical anomalies of this area are developed in close relation to the altered zones confirmed on the surface. At Tulasewa, geochemical anomalies are distributed not directly over the altered zone, but in the periphery. It is not clear whether this is caused by subsurface alteration or false anomaly by secondary dispersion. Notable geochemical anomaly was not detected associated with the Korokitu Altered Zone.

Many of the anomalous zones have been drilled by Amoco, but the unexplored zones with poly-component anomalies, namely the Vasilaulau and Waidolo Zones are selected for future prospecting.

The extracted anomalies and anomalous areas are largely arranged in the WNW-ESE direction and this is inferred to reflect the macro geologic structure of the region.

Comparing the data of this area to those of the B soil horizon of the Tavua Caldera, the gold producing area, the Cu, Pb, Zn contents of this area are somewhat smaller as seen in the following table. The data for the Tavua area in this table have been quoted from the Report of the First Phase Survey of this project. The original data have been recalculated by anti-logarithmic figures after eliminating the singular values (abnormally high values).

Contrast of soil Assay between Tavua Caldera and Sigatoka Area

	Number of Samples		Average		Maximum		Minimum		unit
	Tavua	Siga'	Tavua	Siga'	Tavua	Siga'	Tavua	Siga'	
Au	56	660	85.5	2.6	*3420	20	<1	<5	ppb
Ag	57	660	-	-	<0.2	<0.2	<0.2	<0.2	ppm
Cu	52	660	131	36	406	500	59	2	ppm
Pb	52	660	9	2	120	250	<2	<1	ppm
Zn	52	660	89	81	154	800	32	1	ppm
As	56	660	6.4	0.6	*500	10	1	<1	ppm
Sb	55	660	0.2	0.4	*58.0	4.0	<0.2	<0.2	ppm
Hg	52	660	42	28	*5800	140	10	10	ppb
Mo	51	660	3.1	0.60	*4190	5	<1	<1	ppm

Siga' : Sigatoka

* : abnormal high value(excluded from calculation)

Chapter 4 Gravity Survey

4-1 Survey Methods

As shown in Figure 2-4-1, the process of gravity survey is largely grouped into "field survey", "data processing" and "analysis & interpretation".

4-1-1 Field Survey

(1) Gravity measurements

a. Stations

Gravity measurement was carried out at 838 stations in an area of about 8,400 km^2. The locations of the stations are shown in the Annexed Figure 16 and Figure 2-4-2. In these figures, the locations of the 517 stations in northern Viti Levu used during the first phase of this project carried out in 1990 are also shown. The 838 stations of this year are numbered 1 - 787 and 901-951. The 51 stations 901-951 are those in the "Sigatoka" area which were not included in the original plan, but added during the survey.

The density of measurements is one station every 5 km^2 in "Sigatoka" and every 10 km^2 in other areas.

b. Instrumentation

Two sets of LaCoste G gravimeters were used for field measurements. This gravimeter was selected considering its extremely good transportability, ease of operation and accuracy of measurements. The specifications of the LaCoste gravimeters used are as follows.

Gravity meter No.	G-178	G-204
Year of manufacture	Feb., 1968	May, 1969
Operating range	0~7,344.88 mgal	0~7,261.53 mgal
Accuracy	0.02 mgal	
Size	14 ×15×20 cm	
Weight	8.6 kg	
Power source	12 V battery	
Manufacturer	LaCoste & Romberg(USA)	

The milligal constant (K) and scale constant (κ) for the range used in this survey are as follows.

Gravimeter No.	Counter reading	Milligal constant	Scale constant
G-178	1800	1884.20	1.04760
	1900	1988.96	1.04770
	2000	2093.73	1.04780
	2100	2198.51	1.04790
G-204	1900	1966.54	1.03620
	2000	2070.16	1.03640
	2100	2173.80	1.03650

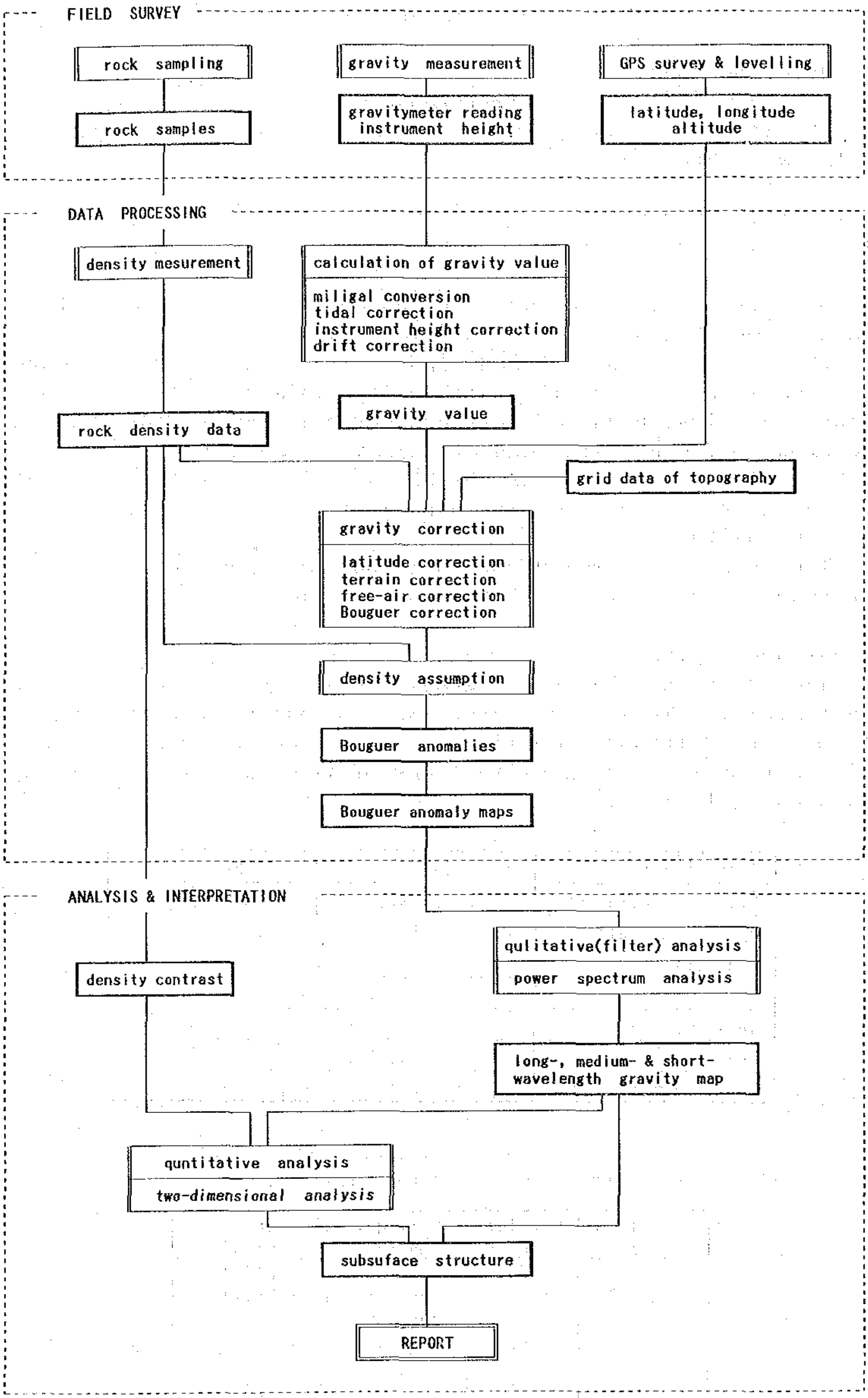

Fig. 2-4-1 Gravity Survey Procedures

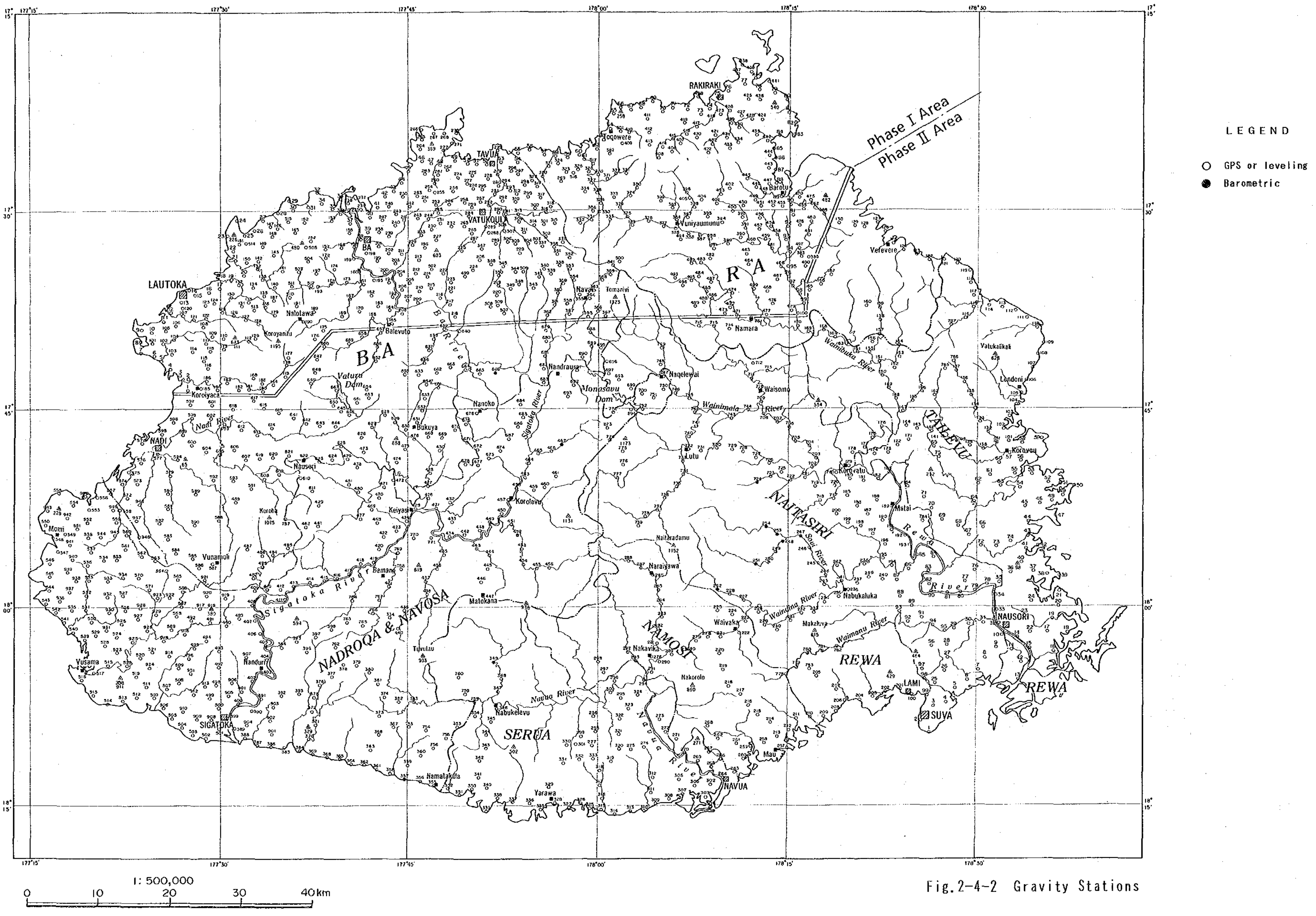

Fig.2-4-2 Gravity Stations

c. Gravity base stations and reference stations

The base stations are the starting and termination points of each survey route. The gravity survey was carried out in Suva, Sigatoka and Nadi areas. A base station was established in each of these areas. The gravity values of these base stations are listed below.

St.No.	Gravity value	Location
4000	978,604.677 mgal	Front of Capricorn Apartment Hotel, Suva
5000	978,614.426 mgal	Sigatoka Hotel compound, Sigatoka
6000	978,551.979 mgal	Entrance of Nadi Hotel New Bldg., Nadi

The accurate location of the base stations are shown together with photographs in the Annex.

The following three reference stations were used for determining the gravity values of the base stations. Jezek(1976) was used for the gravity values of the reference stations.

St.No.	Elev.	Lat.	Long.	Gravity value	Location
189-63	17.8m	18° 07.00'S	178° 27.5'E	978,599.56mgal	MRD, Suva
189-69	5.0m	17° 45.50'S	177° 25.0'E	978,532.11mgal	Nadi Airport
189-70	5.0m	17° 45.70'S	177° 25.0'E	978,532.11mgal	Nadi Airport

MRD:Mineral Resources Department

Reference station 189-63 was used for determining the gravity of base station 4000, 189-69 and 189-70 for 5000 and 6000 respectively.

(2) Leveling

The elevation of the stations was mainly determined by GPS (Global Positioning System) static survey which uses the signals from satellites. This was augmented by conventional leveling using auto-level and altimeter.

a. Instrumentation

Three sets of 4000ST GPS surveyers (Trimble Navigation Ltd.), one WILD NA20 automatic level and two Paulin precision altimeters were used for leveling.

b. GPS survey

GPS relative positioning was employed. In this method, the position of the station is determined by receiving the satellite signals simultaneously at the base and the measurement stations and then calculating the position of the station relative to that of the base. By this relative positioning of the GPS static survey, accuracy of several centimeters can be obtained by one hour observation and of less than a meter by 20 to 30 minutes observation.

The GPS base station was established on the roof of the Colonial War Memorial Hospital in Suva, the roof of Sigatoka Hotel in Sigatoka and in the PWD (Public Works Department) compound in Nadi. The elevation of the GPS base stations was determined by relative positioning with the known elevation base stations shown in the following table.

St. name	Elevation	Latitude	Longitude
Nacovu Tri.	68.572 m	18° 08' 35.28"S	178° 26' 24.43"E
Nandai Tri.	45.928 m	18° 09' 06.85"S	177° 30' 53.19"E
Loa Tri.	33.802 m	17° 39' 04.43"S	177° 23' 37.39"E
Loa GPS	28.364 m	17° 39' 03.10"S	177° 23' 35.60"E

For determining the elevation of the base stations, satellite observation was carried out for one hour. For ordinary measurements, 10 minutes to one hour observation was necessary depending on the number of available satellites and the location.

From GPS survey, latitudes and longitudes based of "WGS (World Geodetic System)-84" ellipsoid are obtained and these were converted to coordinates based on "International" ellipsoid during data processing. Of the 838 stations established, 731 were positioned by GPS method.

c. <u>Leveling</u>

The 96 stations with relatively small differences of elevation along the road in Sigatoka and Nadi areas were positioned by conventional leveling the automatic level. When the stations were included in the topographic map of "Clark 1880" ellipsoid, the latitudes and longitudes were converted to those of "International" ellipsoid.

d. <u>Altimeter measurements</u>

Precision altimeters were used for the determination of elevation at 11 localities where use of GPS and levels was hindered by topography, vegetation and other factors. These stations are shown by black circles on Figure 2-4-2. The coordinates of these stations were read from topographic maps as in the case of stations positioned by level.

(3) Sampling

Rock samples for density measurements were collected throughout the survey area with due consideration to the stratigraphy, lithology and other relevant factors. The number of collected samples amounted to 108 and the localities are shown in Figure 2-4-3.

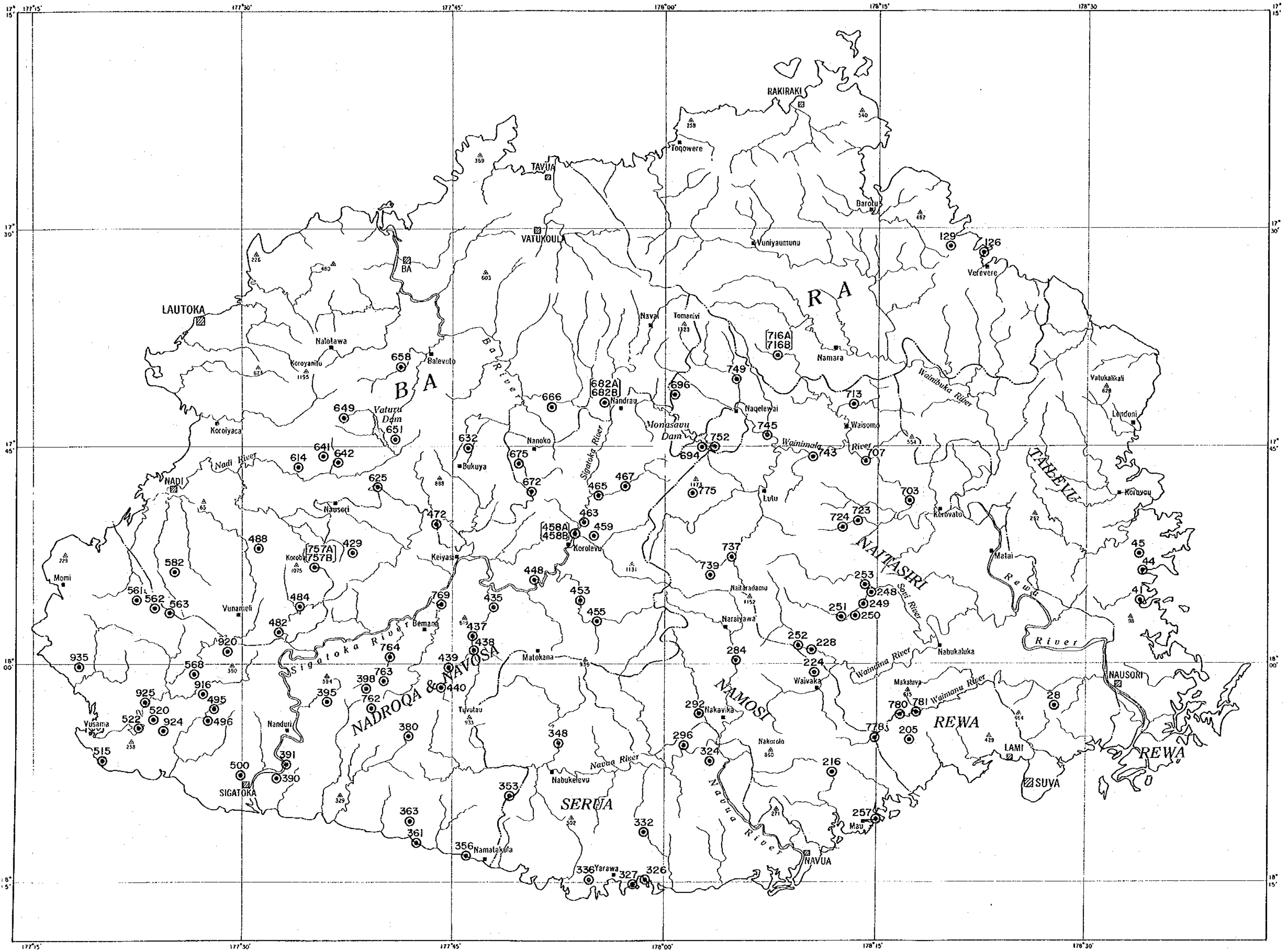

LEGEND

123 Sample No.

◉ Location

1 : 500,000

0 10 20 30 40km

Fig.2-4-3 Density Sample Location

4-1-2 Data Processing

Data processing for gravity survey largely consists of the following two parts.

① Calculation of gravity values from the dial readings (gravity value calculation).

② Calculation of Bouguer anomalies (gravity reduction).

These are processed on the basis of the data files prepared for each station.

(1) Preparation of original data files

The original data file contains; station number, date and time of measurement, gravimeter dial reading, instrument height, latitude, longitude, elevation, terrain correction of "neighbour", code number of gravimeter, leveling method and terrain correction of "close" relevant for subsequent processing. These data are stored in a floppy disk. The format of an original data file is shown in Table 2-4-1.

(2) Calculation of gravity values

In order to calculate the gravity values from the dial readings, "milligal conversion", "tidal correction", "instrument height correction" and "drift correction" are carried out.

<u>a. Milligal conversion</u>

This process converts the dial readings to milligal value. In the case of LaCoste gravimeters, the scale constant slightly changes with the stretching of the spring. Therefore, this conversion is carried out using the milligal constant(K) and scale constant(κ) designated for every 100 units of the reading value.

The basic equation for the conversion is as follows.

$$Vr = K + (R - R_0) \times \kappa \qquad (4\text{-}1)$$

Vr: Measured value in milligal

R : Gravimeter readings

R_0: Under 100 omitted from R

For example, if R is 2,062.364, R0 is 2,000, K is 2,093.73, scale constant(κ) is 1.04780. Therefore, the equation will be,

$$Vr = 2,093.73 + (2,062.364 - 2,000) \times 1.04780 \qquad (4\text{-}2)$$

<u>b. Tidal correction</u>

The observed gravity values vary periodically within the range of 0.2 mgal because of the following two factors. The correction for these variations is the tidal correction.

① Periodic variation by tidal force.

② Very small deformation of the earth by the tidal force

Table 2-4-1 Original Data File Format

Column	Format	Contents		Remarks
1−5	A5	Area name		FIJI
6−7	A2	Sign of base station		ST : base station
8−13	I6	Station No.		
14−15	I2	Year	Observed date	1990→90
16−17	I2	Month		Dec.→12
18−19	I2	Day		5th→05, 15th→15
20−21	I2	Hour		9→09, 15→15
22−23	I2	Minute		6→06, 36→36
24−31	F8・3	Reading value		
32−36	F5・2	Instrument height(m)		
37−44	F8・3	Elevation(m)		
45−52	F8・2	Latitude		South lat. 17°36.91′→ 173691
53−61	F9・2	Longitude		East long. 177°27.26′→1772726
62−66	F5・2	Onshore "neighbour" terrain correction value		ρ =2.0 g/cm³
67−71	F5・2	Offshore"neighbour" terrain correction value		ρ =1.0 g/cm³
72−73	I2	Gravimeter No.		Code No. of LaCoste gravimeters 1 : G-150, 2 : G-178, 3 : G-204, 4 : G-206, 5 : G-236, 6 : G-283, 7 : G-286, 8 : G-365, 9 : G-366, 10 : G-579
74	I1	Blank		
75−76	I2	Leveling method		0 : leveling, 6 : GPS
77−80	F4・2	"close" terrain correction value		ρ =2.0 g/cm³

(earth tide).

This force is expressed by equation(4-3).

$$U = \frac{3}{2} \cdot G \cdot M \frac{a}{r^3} \{3(\sin^2\delta - \frac{1}{3}) \cdot (\sin^2\phi - \frac{1}{3}) + \sin 2\delta \cdot \sin 2\phi \cdot \cos\theta + \cos^2\delta \cdot \cos^2\phi \cdot \cos 2\theta\} \quad (4\text{-}3)$$

U : Tidal force of celestial bodies

G : Gravitational constant

M : Mass of celestial bodies (sun, moon etc.)

a : Distance from the center of the earth to the station (earth's radius)

ϕ : Latitude of the station

r : Distance between the earth and the celestial bodies

δ : Declination of the celestial bodies (angle from the equator)

θ : Hour angle of the celestial bodies (angle between terrestrial and celestial meridian plane)

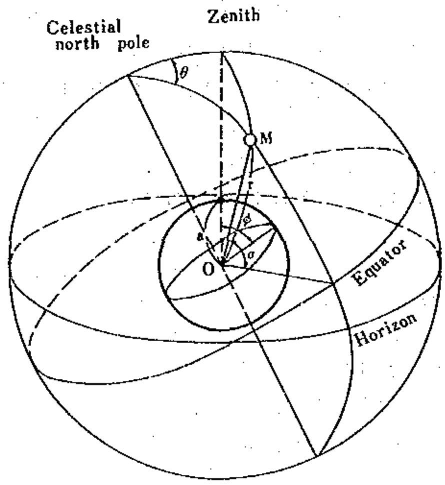

The tidal force of the sun and moon is overwhelmingly greater than that of other celestial bodies. Therefore, the correction for these two bodies will suffice for gravity prospecting.

The gravity variation caused by earth tide has the same sense as that by the tidal force and the rate of change differs somewhat by the elasticity of the rocks of the area, but it is in the order of 20 % of that caused by tidal force. Therefore, in normal tidal correction, the tidal force by the sun and moon is multiplied by 1.20 which is called the tidal constant.

c. Correction for instrument height

This correction is made in order to compensate for the difference of the height for leveling and gravity measurements.

The correction is done by using the vertical normal gravity gradient on the surface of the ellipsoid of revolution(0.3086 mgal/m) on equation(4-4).

$$Vhi \fallingdotseq \frac{2\gamma_0}{R} hi \fallingdotseq 0.3086\ hi \qquad (4\text{-}4)$$

Vhi: Instrument height correction value
γ_0 : Normal gravity
R : Distance from the earth's center to the station
hi : Height from the leveled point on the earth's surface to the top of the gravimeter

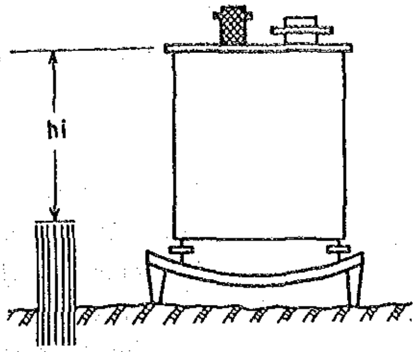

d. Drift correction

The drift is the variation of reading values of the gravimeter caused by the stretching of the spring. The value of the drift is roughly proportional to time. The correction for this drift is done by time-proportional allotment of the closed error for each station. The variation of readings are caused not only by drift, but also by the changes of temperature, atmospheric pressure and mechanical shock during transportation. In practice, these changes are also corrected by this process.

e. Calculation of gravity values

All corrections for measured gravity values are expressed by equation(4-5).

$$Vc = Vr + Vt + Vhi + Vd \qquad (4\text{-}5)$$

Vc: Corrected gravity value
Vt: Tidal correction value
Vd: Drift correction value

The corrected gravity value Vc shows the relative value of gravity and not the absolute value of gravity. The gravity value of each station is calculated by obtaining the difference of the corrected gravity values between the station and the base station and then adding the gravity value of the base station to this difference. The gravity value of the base station is obtained by separate measurement between the base station and the reference station where the gravity value is known.

(3) Gravity reduction

The process of calculating the Bouguer anomaly values is called the gravity reduction and it consists of "latitude correction", "terrain correction", "atmospheric correction", "free air correction" and "Bouguer correction".

a. Latitude correction

This correction is done by subtracting the standard gravity of the earth from the gravity value. The standard gravity is given as a function of the latitude and normal gravity γ_0 of equation(4-6) is presently used as the standard gravity.

$$\gamma_0 = \frac{a\gamma_E\cos^2\phi + b\gamma_P\sin^2\phi}{\sqrt{a^2\cos^2\phi + b^2\sin^2\phi}} \qquad (4\text{-}6)$$

a : Equatorial radius of the ellipsoid of revolution(6,378.14 km)

b : Polar radius of the ellipsoid of revolution(6,356.75 km)

γ_E: Equatorial normal gravity of the ellipsoid of revolution (978.032 gal)

γ_P: Polar normal gravity of the ellipsoid of revolution(983.218 gal)

However, for practical gravity prospecting, the following approximation is used.

$$\gamma_0 = 978031.85(1+0.005278895\sin^2\phi + 0.000023462\sin^4\phi)\ \text{(mgal)} \qquad (4\text{-}7)$$

b. Terrain correction

This correction is made in order to correct the effect of the topographic relief of the vicinity of the stations on gravity values. It is done in a fashion by which high reliefs are shaved off and depressions are buried and a flat surface is assumed. The correction for both cases is positive. The correction for flat surface is 0 mgal and for areas with rugged relief, it may reaches tens of milligals.

For the present survey, the range of terrain correction was set for a radius of 60 km and the area was divided into five correction zones as follows.

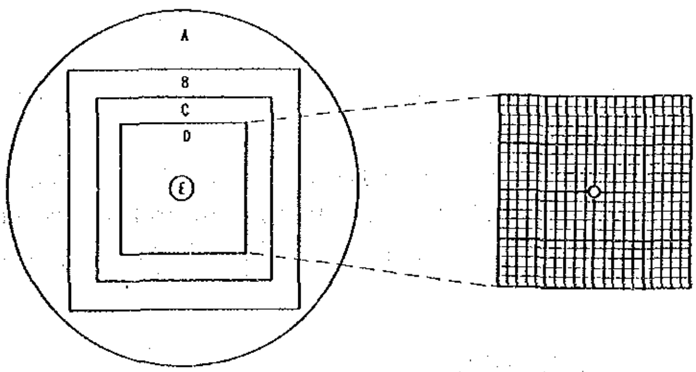

Terrain Correction Concept

Items of Terrain Correction

Zone	Range of correction	Grid interval	Correction type
A	60km radius - zone B	4 km × 4 km	Far
B	32km × 32km - zone C	1 km × 1 km	Medium
C	8 km × 8 km - zone D	250m × 250m	Near
D	1 km × 1 km - zone E	50m × 50m	Neighbour
E	20m radium from station		Close

The effect of topography is stronger near the stations and is inversely proportional to the square of the distance from the station. Therefore, the grid is set densely closer to the station. The topographic elevation grid data which were read every 50 m in the 1/50,000 topographic maps were used for the correction of Zones A-D. For Zone E, topographic profile of 20 m radius from the sketched station was used for calibration.

c. Atmospheric correction

This is done in order to correct the effect of the atmosphere to gravity measurement. The atmospheric pressure will be integrated to a height of 50 km above the station using the atmospheric density distribution based on standard atmospheric model. The correction value decreases exponentially with altitude. The variation of the correction values, however, can be appproximated by a linear function for altitude below 3 km. And equation(4-8) is usually used for this correction.

$$\delta g_A = 0.87 - 0.0965 \times 10^{-3} H \qquad (4\text{-}8)$$

δg_A: Atmospheric correction value(mgal)

H : Elevation of the station(m)

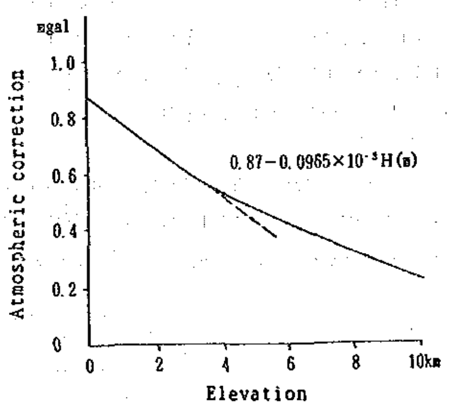

d. Free air correction

The vertical gravity gradient near the earth's surface is -0.3086 mgal/m, and thus the gravity decreases with height. The free air correction corrects the effect of elevation for each station.

$$\delta g_F \fallingdotseq \frac{2\gamma_0 H}{R} \fallingdotseq 0.3086 H \qquad (4\text{-}9)$$

δg_F : Free air correction value
γ_0 : Normal gravity
R : Distance from the earth's center to the station
H : Elevation from the geoid

The value defined by equation(4-10) is called the free air anomaly.

$$\Delta g_F = g - \gamma_0 + \Sigma \delta g_T + 0.3086H \quad (4\text{-}10)$$

Δg_F : Free air anomaly
g : Gravity value
$\Sigma \delta g_T$: Terrain correction value

e. Bouguer correction

The difference of the gravity values measured at different elevations corresponds to the attraction of the material (rocks) which exists between the elevations of the stations. Bouguer correction eliminates this difference by setting a datum plane and eliminating material between the datum and a parallel plane passing through each station. Usually geoid is used as the datum. A homogeneous circular slab is assumed to exist between the geoid and a parallel plane including the station for the correction equation(4-11). The radius of this slab is set at 60 km, the same as the range of terrain correction.

$$\begin{aligned}\delta g_B &= -2\pi G \rho (A + H - \sqrt{A^2 + H^2}) \\ &\fallingdotseq -0.0419\rho (A + H - \sqrt{A^2 + H^2}) \quad (4\text{-}11)\end{aligned}$$

δg_B : Bouguer correction value
G : Gravitational constant
ρ : Density, average density of rocks between the geoid and earth's surface
A : Circular slab radius (60 km)
H : Station elevation

f. Bouguer anomaly values

The values obtained by correcting the gravity values for latitude, terrain, atmosphere, free air and Bouguer are called the Bouguer anomalies and are expressed by equation(4-12).

$$\Delta g_B = g - \gamma_0 + \Sigma \delta g_T + 0.87 - 0.0965 \times 10^{-3} H + 0.3086H - 0.0419\rho (A + H - \sqrt{A^2 + H^2}) \quad (4\text{-}12)$$

Δg_B: Bouguer anomaly value

The Bouguer anomaly is defined at the earth's surface and the value varies by the density used for the Bouguer and terrain corrections. Thus the Bouguer anomaly contains information not only on the density structure below the geoid but also the difference of the real and the assumed density used in correction for the rocks between the geoid and the surface.

Tables of relevant data regarding this gravity survey are attached in the Appendices. These data include; location (coordinates and elevation) of stations, gravity values, various correction values, normal gravity values and Bouguer anomalies, and Bouguer anomalies for six different assumed density values.

(4) Preparation of gravity maps

The Bouguer anomaly value of each station was converted to grid point value on rectangular coordinates. This was done in order to draft Bouguer anomaly map using a plotter and to obtain gravity values for filter analysis.

La Porte(1962) method was used for calculating the values for the grid points because the reproducibility of the Bouguer anomaly for each station is very good by this method. The grid interval of 1 km was used and the grid point values were calculated only when more than six stations were included within a range of 10 km radius with over 240 degree angle with the center at the grid point. Three types of Bouguer anomaly maps were prepared with correction densities of 2.40, 2.50 and 2.67 g/cm³.

4-1-3 Analytical methods

(1) Density measurement of rock samples

The density of the collected samples was measured by the following formula.

$$\text{Natural dry density} = \frac{W_1}{W_2 - W_3} \qquad (4\text{-}13)$$

$$\text{Wet density} = \frac{W_2}{W_2 - W_3} \qquad (4\text{-}14)$$

W_1: Weight in air of samples left in a room (normal temperature) for several days (naturally dried).

W_2: Weight in air of samples immersed in water for 24 hours under natural atmospheric pressure and the surface was wiped with cloth.

W_3: Weight in water after immersion under natural atmospheric pressure for 24 hours.

(2) Gravity analysis

a. Power spectral analysis

This method is used with the objective of separating the long- and medium-wavelength anomalies caused by deep-seated structures and the short-wavelength anomalies caused by shallow structures.

The power spectrum P_{mn} is expressed by the equation(4-15), if the relief of the density boundary is irregular when the Bouguer anomalies are expanded by Fourier series.

$$\ln P_{mn} = C - 4\pi D\sqrt{\left(\frac{m}{L_1}\right)^2 + \left(\frac{n}{L_2}\right)^2} \qquad (4\text{-}15)$$

C : constant

D : Average depth of the density boundary

L_1, L_2: Lengths of the sides of rectangle

m, n : Wave numbers

When data are plotted with $\ln P_{mn}$ on the ordinate and $\sqrt{(m/L_1)^2+(n/L_2)^2}$ on the abscissa, two or more lines with different gradients can be drawn through these plots. According to the power spectrum theory, each of these lines represents density boundaries at different depths.

The linearity of the smaller frequency groups indicates deep boundary and that of the larger frequency groups shallow boundary.

b. Profile analysis

The profile analysis is a quantitative analysis aimed at constructing a two dimensional model of the subsurface structure which would result in gravity anomalies approximating most closely those measured in the area. The gravity anomalies of the model are calculated by the following Talwani et al.(1959) equation.

$$g = 2G\Delta\rho\Sigma Z_i \qquad (4\text{-}16)$$

$$Z_i = A_i \sin\phi_i - \cos\phi_i\left[\theta_i - \theta_{i+1} + \tan\phi_i \log\frac{\cos\theta_i(\tan\theta_i - \tan\phi_i)}{\cos\theta_{i+1}(\tan\theta_{i+1} - \tan\phi_i)}\right] \qquad (4\text{-}17)$$

g : Gravity anomaly value

G : Gravitation consttant

$\Delta\rho$: Density contrast($\rho_2-\rho_1$)

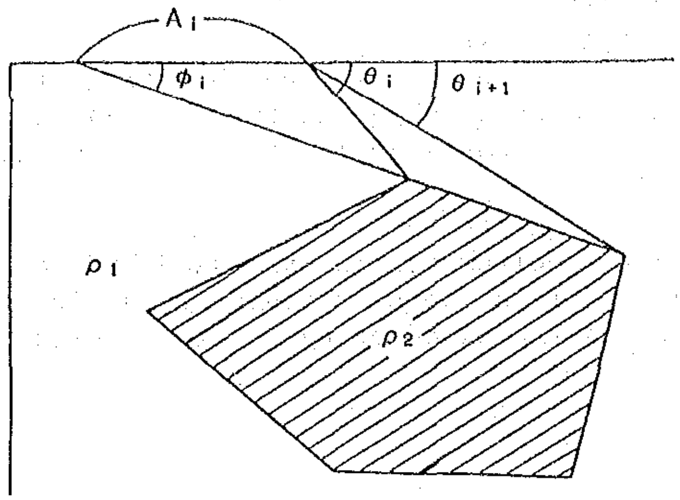

Schematic analysis of two-dimensional density structure by Talwani's method

When the subsurface density structure can be approximated by two-layered model, unique solution can be obtained by; disignating a density contrast and a control depth, and then gradually altering the shape of the density boundary thus approximating the calculated values closer to the measured values. This method is very effective when the subsurface density structure can be approximated by two-layered structure, and good solutions can be obtained in short time.

During this survey, two-layered model analysis was used for the short-wavelength and medium-wavelength gravity anomalies.

4 - 2 Survey Results

4-2-1 Density measurements

The results of the density measurements of the 108 samples are shown in Table 2-4-2 and the average wet density of is shown by formations and rocks in Table 2-4-3. The average wet density of the 108 samples is 2.53 g/cm^3. The average density of the 38 samples measured during Phase I of this project is 2.50 g/cm^3 (Table 2-4-4) and that of the 266 samples in Rodda and Deberal (1966) is 2.64 g/cm^3.

The formations with relatively high density are the following (Table 2-4-3).

Volcanic rocks of the Ba Volcanic Group	2.65 g/cm^3
Cuvu Sedimentary Group	2.57 g/cm^3
Koroimavua Volcanic Group	2.56 g/cm^3

Coro Plutonic Suite	2.66 g/cm³
Wainimala Group	2.56 g/cm³
Yavuna Group	2.71 g/cm³

On the other hand, Formations with relatively low density are as follows.

Verata Sedimentary Group	2.30 g/cm³
Sedimentary rocks of the Ba Volcanic Group	2.12 g/cm³
Navosa Sedimentary Group	2.40 g/cm³
Nadi Sedimentary Group	2.43 g/cm³
Medrausucu Group	2.31 g/cm³
Tuva Group	2.49 g/cm³

This can be summarized as follows.

① The lithology affects the density more than the formations. With the exception of limestone, the sedimentaryrocks generally have lower density, while the volcanic and intrusive rocks have high density.

② Sedimentary rocks in older formations tend to have higher density.

③ With the exception of gabbro of the Coro Plutonic Suite, the oldest Yavuna Group has the highest density.

④ In the Wainimala Group, the density of the sedimentary rocks (18 samples, 2.49 g/cm³) is lower than that of the volcanic rocks (25 samples, 2.61 g/cm³).

⑤ In the Ba Volcanic Group, the difference between the density of the sedimentary rocks (7 samples, 2.12 g/cm³) and volcanic rocks (9 samples, 2.65 g/cm³) is very large.

The density of a sample from the Ra Sedimentary Group was measured last year during the first phase of this project, it was 1.60 g/cm³, and other existing documents report 2.35 g/cm³(3 samples) by previous measurement.

The average density of each formation is as follows.

Verata Sedimentary Group		2.25± g/cm³
Ba Volcanic Group	sedimentary rocks	2.10± g/cm³
" "	volcanic rocks	2.70± g/cm³
Koroimavua Volcanic Group		2.60± g/cm³
Navosa Sedimentary Group		2.40± g/cm³
Nadi Sedimentary Group		2.40± g/cm³
Ra Sedimentary Group		2.20± g/cm³
Medrausucu Group		2.35± g/cm³
Tuva Group		2.45± g/cm³
Colo Plutonic Suite	tonalite, diorite	2.65± g/cm³

Table 2-4-2 Rock Density(1/2)

Staratigraphic units	Sample NO.	Code	Rock name	Density (g/cm³) Naturay dry	Wet
Verata Sedimentary Group	41	Vnc	Siltstone	2.45	2.47
	44	Vnc	Tuffceous Siltstone	1.71	1.98
	45	Vnc	Tuffceous Siltstone	2.44	2.46
Ba Volcanic Group	126	Bnk	Basalt	2.48	2.50
	129	Bnk	Basalt	2.68	2.68
	467	Bvk	Siltstone	2.14	2.21
	625	Bs	Basalt	2.66	2.67
	666	?	Basaltic Tuff	2.12	2.22
	672	Bvk	Hornblende Andesite	2.38	2.46
	675	Bnk	Siltstone	2.14	2.21
	682A	Bnu-Bnk	Siltstone	1.78	1.93
	682B	Bnu-Bnk	Basalt	2.54	2.56
	694	Bvk	Siltstone	1.96	2.12
	696	Bnk-Bnu	Basalt	2.73	2.73
	716A	Bvk	Sandstone	1.80	1.99
	716B	Bvk	Tuffceous Sandstone	2.04	2.18
	749	Bnk-Bnu	Basalt	2.96	2.96
	752	?	Dacite	2.41	2.43
	775	Bnk	Basalt	2.82	2.82
Cuvu Sedimentary Group	515	Cu	Sandstone	2.53	2.57
Koroimavua Volcanic Group	641	Ks	Hornblende Andesite	2.37	2.39
	642	Ks	Basalt	2.62	2.63
	649	Ks	Hornblende Andesite	2.43	2.48
	651	Ks	Basalt	2.70	2.71
	658	Ks	Basalt	2.58	2.60
Navosa Sedimentary Group	398	Nvv	Sandstone	2.23	2.33
	435	Nvs	Tuffaceous Siltstone	2.25	2.35
	472	Nva	Andesite	2.29	2.39
	762	Nvv	Sandstone	2.51	2.53
Nadi Sedimentary Group	632	Nd II	Basaltic Tuff	2.37	2.43
Medrausucu Group	28	Msm	Sandstone	1.68	1.92
	257	Mv	Hornblende Andesite	2.41	2.47
	292	Mnv	Sandstone	2.40	2.47
	296	Mnv	Tuff	1.96	2.12
	324	Mnv	Sandstone	2.33	2.40
	780	Mnm	Andesite	2.45	2.47
Tuva Group	482	Tc	Sandstone	2.28	2.30
	484	Tc	Siltstone	2.46	2.49
	763	Tt	Sandstone	2.38	2.44
	764	Tt	Limestone	2.67	2.69
	769	Tt	Sandstone	2.45	2.49
	920	Tt	Siltstone	2.50	2.52
Colo Plutonic Suite	216	Cg	Gabbro	2.80	2.80
	248	Ct	Granodiorite	2.56	2.58
	249	Ct	Granodiorite	2.60	2.61
	250	Ct	Granodiorite	2.56	2.58
	251	Ct	Granodiorite	2.62	2.62
	253	Ct	Granodiorite	2.61	2.62
	348	Ct	Granodiorite	2.63	2.63
	363	Ct	Tonalite	2.59	2.59
	453	Cg	Gabbro	2.76	2.77
	455	Cg	Gabbro	2.89	2.89
	458A	Ct	Tonalite	2.63	2.65
	459	Ct	Tonalite	2.31	2.34

Table 2-4-2 Rock Density(2/2)

Staratigraphic units	Sample NO.	Code	Rock name	Density (g/cm^3)	
				Naturay dry	Wet
Colo Plutonic Suite	703	Ct	Granodiolite	2.91	2.91
	724	Ct	Granodiolite	2.68	2.69
	737	Ct	Tonalite	2.80	2.80
	739	Ct	Tonalite	2.82	2.83
	778	Ct	Diorite	2.34	2.38
Wainimala Group	205	Mtt	Propylite (Dacitic)	2.44	2.48
	224	Wnu	Propylite (Basaltic)	2.52	2.56
	228	Wnu	Basalt	2.75	2.76
	252	Wnu	Basalt	2.63	2.63
	284	Wnu	Basalt	2.63	2.65
	326	Wnu	Basalt	2.35	2.37
	327	Wnu	Basalt	2.40	2.42
	332	Wtt	Mudstone	2.40	2.41
	336	Wnu	Basaltic Tuff	2.63	2.64
	353	Wlo	Dacite	2.66	2.66
	356	Wnu	Basaltic Tuff	2.03	2.13
	361	Wnu	Basalt	2.68	2.69
	380	Wnu	Basaltic Tuff	2.75	2.75
	390	Wta	Limestone	2.66	2.67
	391	Wta	Sandstone	2.47	2.49
	395	Wta	Sandstone	2.30	2.39
	437	Wtu	Basaltic Tuff	2.55	2.56
	438	Wtu	Basaltic Tuff	2.66	2.67
	439	Wtu	Siliceous Mudstone	2.20	2.24
	440	Wtu	Dacitic Tuff	2.31	2.37
	448	Wnm	Basalt	2.77	2.77
	458B	Wnm	Hornblende Andesite	2.67	2.67
	463	Wnm	Basalt	2.77	2.77
	465	Wnm	Dacite	2.53	2.54
	495	Wta	Basalt	2.80	2.80
	496	Wta	Siliceous Mudstone	2.58	2.58
	500	Wta	Basalt	2.70	2.70
	520	Wta	Dacite	2.55	2.56
	522	Wta	Propylite (Andesite)	2.69	2.70
	561	Wd(Wnd)	Basalt	2.39	2.40
	562	Wnd(Wd)	Basalt	2.44	2.48
	563	Wd	Siltstone	2.53	2.55
	568	Wta	Basaltic Tuff	2.40	2.41
	614	Wnd	Dacitic Tuff	2.29	2.39
	707	Wnu	Basalt	2.65	2.65
	713	Wwk	Basalt	2.59	2.60
	723	Wnu	Andesite	2.81	2.81
	743	Wnu	Basalt	2.67	2.68
	745	Wla	Basalt	2.52	2.52
	781	Mtt	Basaltic Tuff	2.54	2.56
	916	Wta	Dacite	2.45	2.49
	924	Wta	Dacitic Tuff	2.34	2.39
	925	Wta	Basalt	2.52	2.56
	935	Wta	Limestone	2.68	2.69
Yavuna Group	429	Yvs	Granodiorite	2.70	2.71
	488	Yv	Basalt	2.73	2.74
	582	Yv	Basalt	2.74	2.76
	757A	Yv	Basalt	2.63	2.64
	757B	Yv	Basalt	2.69	2.70

Table 2-4-3 Average Rock Density(Wet)

Age		Staratigraphic	Rock name	Number	Average density(g/cm³)		
Quaternary	Pleistocene	Verata Sedimentary Group	Siltstone	1	2.47	2.30	
			Tuffceous Siltstone	2	2.22		
Neogene	Miocene to Pliocene	Ba Volcanic Group	Basalt	7	2.70	2.65	2.42
			Dacite	1	2.43		
			Hornblend Andesite	1	2.46		
			Siltstone	4	2.12	2.12	
			Basaltic Tuff	1	2.22		
			Sandstone	2	2.09		
		Cuvu Sedimentary Group	Sandstone	1	2.57		
		Koroimavua Volcanic Group	Basalt	3	2.65	2.56	
			Hornblend Andesite	2	2.44		
		Navosa Sedimentary Group	Andesite	1	2.39		2.40
			Tuffceous Siltstone	1	2.35	2.40	
			Sandstone	2	2.43		
		Nadi Sedimentary Group	Basaltic Tuff	1	2.43		
		Medrausucu Group	Andesite	2	2.47		2.31
			Sandstone	3	2.26	2.23	
			Tuff	1	2.12		
		Tuva Group	Limestone	1	2.69	2.49	
			Siltstone	2	2.51		
			Sandstone	3	2.41		
		Colo Plutonic Suite	Gabbro	3	2.82	2.66	
			Granodiorite	9	2.62		
			Tonalite	5	2.64		
		Wainimala Group	Basalt	17	2.61	2.61	2.56
			Propylite	3	2.58		
			Dacite	4	2.56		
Paleogene	Oligocene		Andesite	1	2.81		
			Limestone	2	2.68	2.49	
			Siltstone	1	2.55		
			Sandstone	2	2.44		
			Mudstone	3	2.41		
			Basaltic Tuff	7	2.53		
			Dacitic Tuff	3	2.38		
		Yavuna Group	Granodiorite	1	2.71	2.71	
	Eocene		Basalt	4	2.71		
Average				108	2.53		

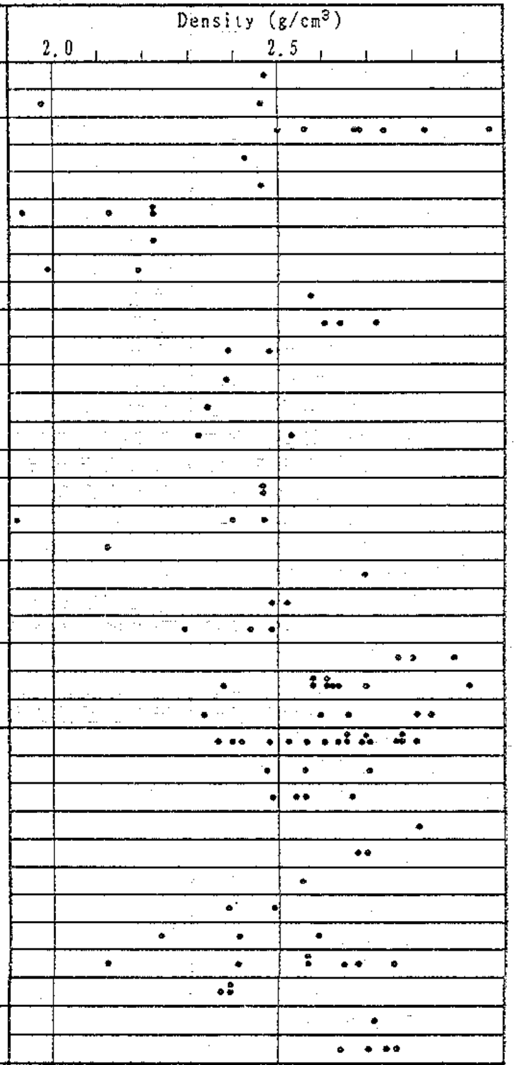

Table 2-4-4 Average Rock Density(Wet) of Phase I Samples

Age		Stratigraphic units	Number	Average density(g/cm³)		
Quaternary	Pleistocene	Verata Sedimentary Group	3	2.09	2.48	2.48
Neogene	Miocene to Pliocene	Ba Volcanic Group	19	2.54		
		Koroimavua Volcanic Group	4	2.72	2.49	
		Navosa Sedimentary Group	1	2.56		
		Nadi Sedimentary Group	1	2.39		
		Ra Sedimentary Group	1	1.60		
		Colo Plutonic Suite	1	2.78		
Paleogene	Oligocene	Wainimala Group	5	2.49		
	Eocene	Yavuna Volcanic Group	3	2.68		
Average			38	2.50		

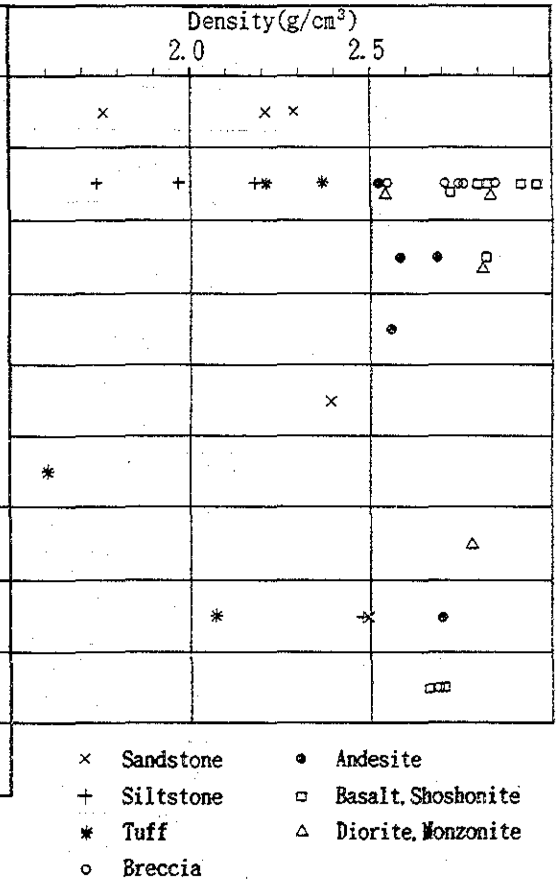

Table 2-4-5 Average Rock Density from Existing Data

Age		Stratigraphic units	Number	Density (g/cm³)		
Quaternary	Pleistocene	Verata Sedimentary Group	1	2.50	2.54	2.47
Neogene	Miocene to Pliocene	Ra Volcanic Group	46	2.54		
		Navosa Sedimentary Group	1	2.10	2.36	
		Nadi Sedimentary Group	1	2.46		
		Ra Sedimentary Group	3	2.35		
		Medrausucu Group	23	2.37		
		Colo Plutonic Suite	89	2.74		
		Tuva Group	2	2.50		
Paleogene	Oligocene	Wainimala Group	100	2.69		
Average			266	2.64		

(compiled a part of data from Rodda P. and Deberal R., 1966)

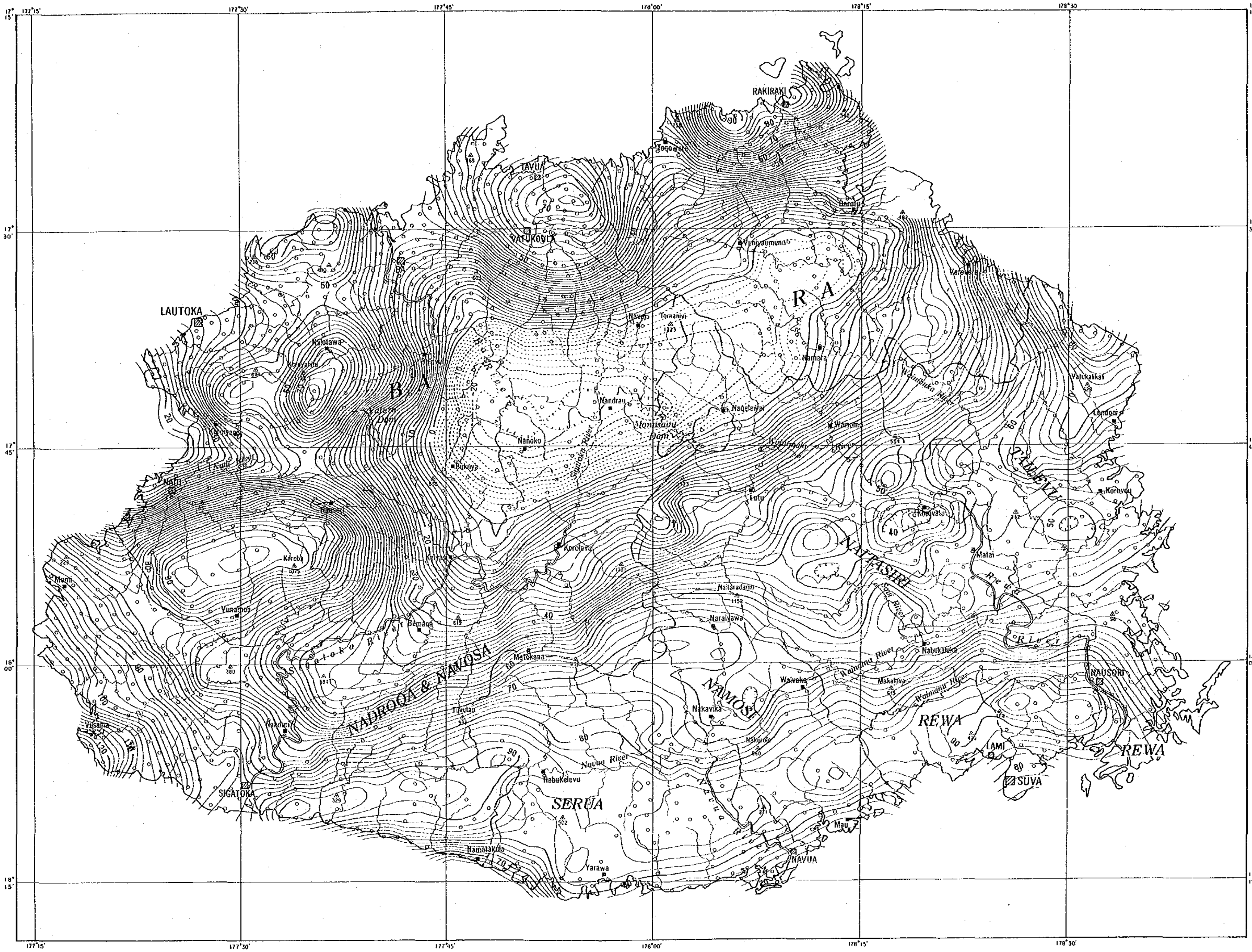

LEGEND

Contour inteval : 2mgal

1: 500,000

0 10 20 30 40km

Fig.2-4-4 Bouguer Anomaly Map(ρ=2.40 g/cm^3)

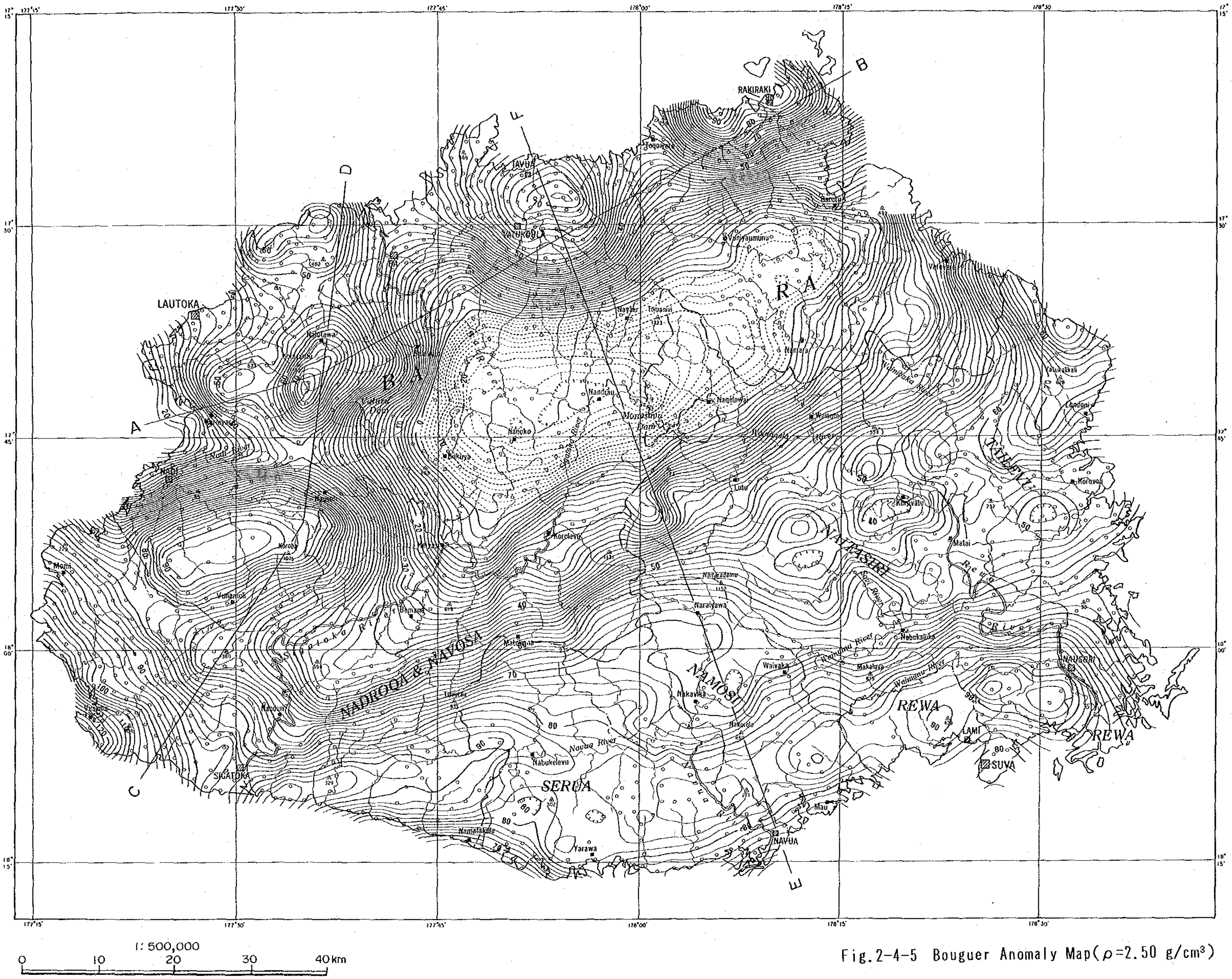

LEGEND

Contour inteval : 2mgal

A – B Section line

Fig. 2-4-5 Bouguer Anomaly Map(ρ=2.50 g/cm^3)

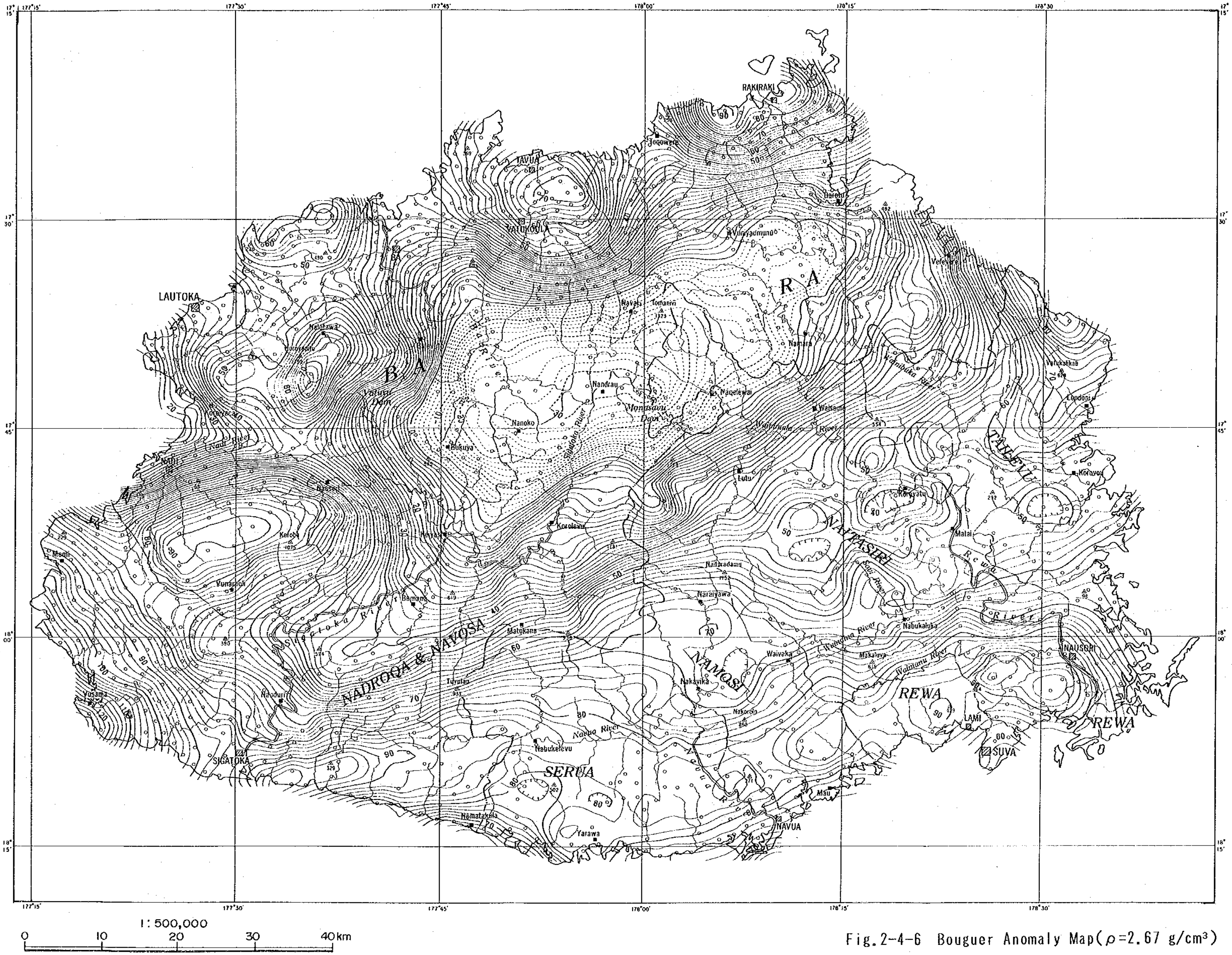

LEGEND

Contour inteval : 2mgal

Fig.2-4-6 Bouguer Anomaly Map(ρ=2.67 g/cm^3)

" " "	gabbro	2.80±	g/cm^3
Wainimala Group	sedimentary rocks	2.45±	g/cm^3
Wainimala Group	volcanic rocks	2.65±	g/cm^3
Yavuna Group		2.70±	g/cm^3

4-2-2 Bouguer anomaly maps

In the Bouguer anomaly map, the contour interval is 2 mgal, and the solid lines and broken lines indicate positive and negative areas of Bouguer anomaly respectively.

Three types of Bouguer anomaly maps were prepared, namely ρ=2.40, 2.50 and 2.67 g/cm^3(Fig. 2-4-4 - 6). During the first phase, Bouguer anomaly map with ρ =2.50 g/cm^3 was selected. This value is again considered to be appropriate for the present interpretation from the density measurements. And this Bouguer anomaly map was selected. Comparing the three types of Bouguer maps, the distribution of the gravity anomalies is similar for all of them. Thus, the interpreted results probably would not differ very much among the three maps. The following interpretation was carried out not only for the survey area of this year, but for the whole Viti Levu Island including the area surveyed last year.

According to the Bouguer anomaly map of the island, there is a low Bouguer anomaly zone, under 0 mgal, in the central part of the island and high anomaly zones exceeding 60 mgal occurs widely in the coastal areas with the exception of the vicinity of Nadi-Lautoka in the northwestern part. The highest Bouguer anomaly (126 mgal) occurs in the southwestern edge of the island and the lowest anomaly (-26 mgal) in the vicinity of Nadrau-Nanoko in the central part of the island. On land, the anomaly is the highest at the southwesternmost part of the island, but it is seen that the anomaly increases seaward.

In the area from northeastern coast to the western part of the island, gravity highs considered to be almost independent are aligned from the east westward; vicinity of Rakiraki, Tavua-Vatukoula, northwest of Ba, southwest of Ba, and southeast of Nadi. On the other hand, in the area from the southeast to southwestern part of the island, the gravity anomalies occur as belts extending in the NE-SW to ENE-WSW direction. The two areas have contrasting gravity features.

Low gravity zone is developed in the central part of the island and extends deeper in the NNE and SW directions.

4-2-3 Filter analysis maps

(1) Results of spectral analysis

The results of the power spectral analysis of the

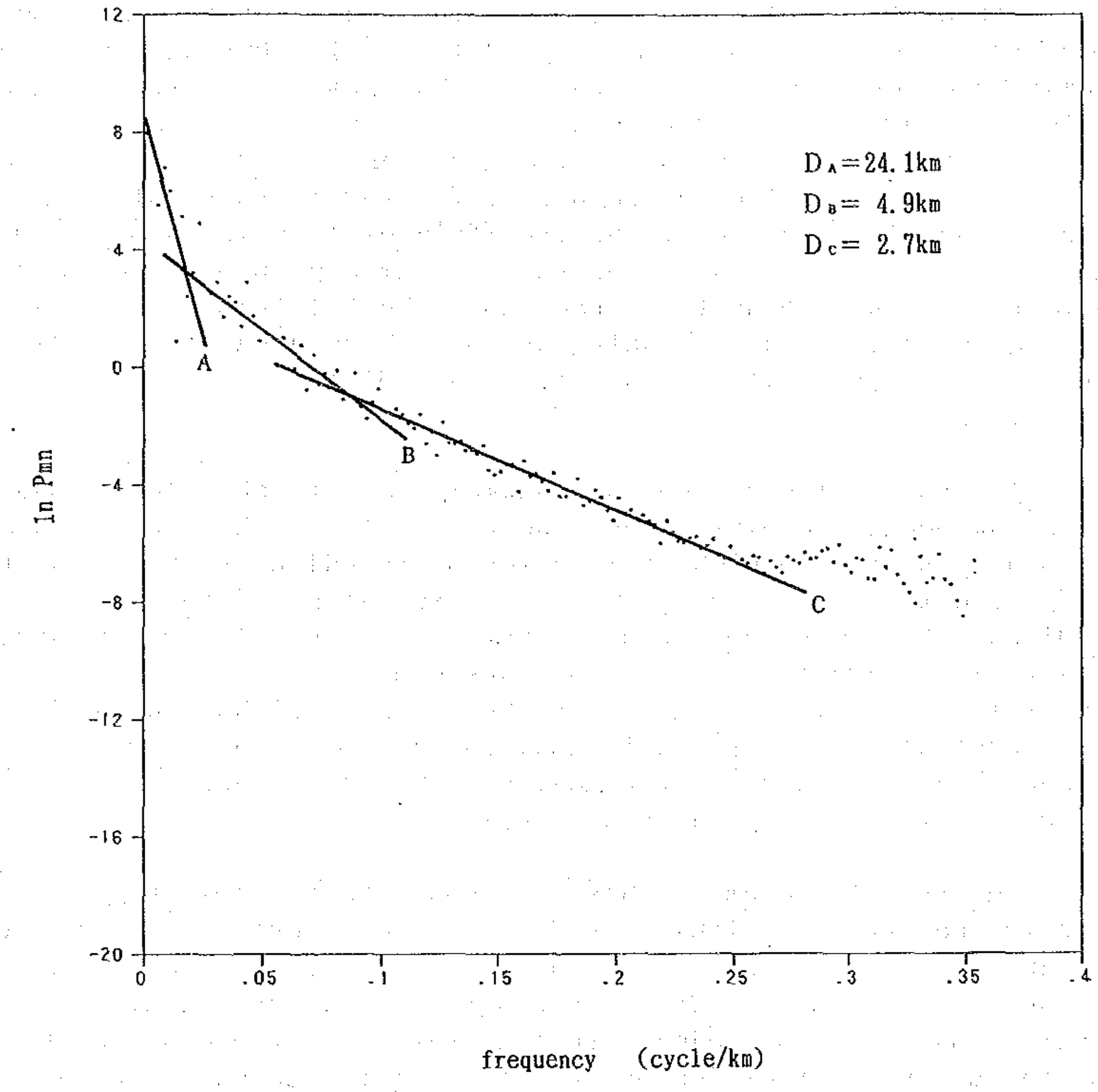

Fig.2-4-7 Power Spectra of Bouguer Anomaly

Bouguer anomaly maps are shown in Figure 2-4-7. In this figure, three lines, A, B and C, with varying gradients can be drawn against the distribution of the power spectra. The following average depth of the density boundary was calculated from these gradients.

A Group	average depth		D_A = 24.1 km
B Group	"	"	D_B = 4.9 km
C Group	"	"	D_C = 2.7 km

From these results, the Bouguer anomalies were separated by the three frequency bands corresponding to the Groups A, B and C. Then long-wavelength gravity map (Fig. 2-4-8), medium-wavelength gravity map (Fig. 2-4-9) and short-wavelength gravity map (Fig. 2-4-10) were prepared. During the first phase of this project carried out last year (1990), the Bouguer anomalies were grouped into two bands, namely the long-wavelength and short-wavelength. The long-wavelength of the first phase would include both the long- and medium-wavelength anomalies of the present phase (1991). And the short-wavelength of the present phase includes somewhat longer wavelength than that of the first phase.

(2) Long-wavelength gravity map

In the long-wavelength gravity map, the contour interval is 2 mgal, and the solid lines and broken lines indicate positive and negative areas of Bouguer anomaly respectively.

There is a center of gravity low indicated by -8 mgal contour near Nandrau situated somewhat in the central part of the island and the Bouguer anomaly increases outward in a radial manner. In the southeastern part of the island, however, there is a maximum zone of Bouguer anomaly to the north of Navua and the anomaly decreases southeastward to the sea. The gradient of the Bouguer anomaly is generally higher in the northern part of the island than in the southern part. This is the long-wavelength gravity features of this island.

Hamburger et al.(1988) estimated, from the seismic velocity data, that the average thickness of the earth's crust in Fiji ranges between 15-20 km, and that of the major islands reaches 25 km. The average depth of the density boundary, 24.1 km, calculated from the power spectra of the long-wavelength gravity anomaly agrees with that calculated from seismic velocity. This indicates that the density boundary reflected in the long-wavelength gravity anomaly corresponds to the Moho Discontinuity.

(3) Medium-wavelength gravity map

In the medium-wavelength gravity map, the contour interval is 2 mgal, and the solid lines and broken lines indicate positive and negative areas of Bouguer anomaly respectively.

Regarding the medium-wavelength gravity anomalies, the gravity features differ significantly to the northwest and southeast of the line joining, Verevere - Monasabu Dam - Korolevu - Sigatoka. This fact indicates the existence of an important tectonic line along this zone. This will be called Verevere-Sigatoka Line.

To the northwest of the Verevere - Sigatoka Line, low gravity anomalies generally prevail, and in this general low gravity area, oval shaped gravity highs occur at four localities; near Rakiraki, Tavua-Vatukoula, southwest of Ba and southeast of Nadi. Another gravity high is found to the northwest of Ba in the Bouguer anomaly map, but this is a relatively small anomaly and is shown in the short-wavelength gravity anomaly map. The above four gravity highs have common features such as the circular to oval shape, steep gravity gradient at the sides, and although the ones to the southwest of Ba and southeast of Nadi are fairly close, these are isolated independent anomalies. The anomaly values of the western two are the same and decreases northeastward to those at Vatukoula and Rakiraki.

The gravity high to the southwest of Nadi agrees well with the distribution of the Yavuna Group which constitutes the basement of the Viti Levu Island. The steep gravity gradient at the side of this anomaly shows the relatively large density contrast between the Yavuna Group and the overlying formations. This again coincides with the fact that the overlying Wainimala Group which has small density contrast is lacking in this area and those with relatively low density groups such as the Navosa, Nadi and Tuva directly overlie the Yavuna Group in this area.

Regarding the gravity high to the southwest of Ba, it agrees partly in the western protrusion with the surface distribution of the Koroimavua Volcanic Group. The three gravity highs, namely those at Rakiraki, Vatukoula and Ba, are located in the center of the volcanic activity which formed the Koroimavua and the Ba Volcanic Groups and thus the relationship with the solidified remnant magma is inferred. These Volcanic activities were mainly basaltic and the solidified magma would probably have formed basic plutonic rocks and the 10-20 km diameter of the anomalies is a reasonable dimension for magma chamber of such nature.

To the southeast of the Verevere-Sigatoka Line, two pairs of high and low gravity belts extending in the ENE-WSW direction occur from inland toward the coast. The two high gravity belts agree very well with the distribution of the Wainimala Group and the Colo Plutonic Suite, and the two low gravity belts with the Medrausucu and Verata Sedimentary Groups. This relationship is harmonious with the densities of the formations. The southeastern high Bouguer anomalies are 20-30 mgal lower than those of the northwestern half, and this is considered to reflect the deeper basement, Yavuna Group, in the southeast. Also the gravity gradient is generally gentler in the southeastern half compared to the northwest and this is believed to be the reflection of the smaller density contrast between the Yavuna and Wainimala Groups, and between the Wainimala and Medrausucu, Verata Groups.

In the southwestern end of the island, contours are elongated in the NNW-SSE direction and is at normal angles to those of the southeastern half of the island. The gravity gradient is gentle, however, and the shape of the distribution is rather similar to that of the southeastern half than the northwestern part. This could be an indication of the possibility that the Verevere-Sigatoka Line does not extend in the WSW direction, but bend at right angles near Sigatoka to the NNW direction.

(4) Short-wavelength gravity map

In the short-wavelength gravity map, the contour interval is 1 mgal, and the areas with anomaly value higher than 2 mgal and lower than -2 mgal are stressed by patterns.

Relatively intense gravity highs, over 2 mgal, and gravity lows, under -2 mgal, occur most frequently along the northeastern to northwestern coast from Rakiraki to Nadi, the area west of Rewa River in the southeastern part of the island also include intense short-wavelength anomalies. Significant short-wavelength anomalies represent large density contrast with adjacent units in shallow subsurface (about 3 km below surface) zones. Thus, they often agree with the distribution of the intrusive bodies, particular strata, caldera and dome structures extracted from SLAR images. The cause of individual short-wavelength anomaly will be discussed in detail in the section "4-3 Discussions".

In the area extending from the central part of the island to the northeastern part where medium-wavelength low gravity zone less than 0 mgal are developed, short-wavelength anomalies with little variation are distributed. Here, it is inferred that thick sedimentary formations of the Ba Volcanic Group and the Ra Sedimentary Group are distributed. The lack of significant short-wavelength anomalies is believed to indicate the small lateral density variation of these formations.

4-2-4 Two dimensional profile analysis

Two dimensional analysis was carried out for three profiles, A - B, C - D, and E - F shown in Figures 2-4-5, 9 and 10. These three profiles pass through almost the same area as the geological cross sections of the First Phase Report. The results of the profile analysis are shown in Figures 2-4-11 to 13. The method of analysis is the automatic one using two-layered model. Deep structure analysis using medium-wavelength anomalies and shallow structure analysis by short-wavelength anomalies were carried out separately. But the results are expressed in one figure.

The upper surface of the Yavuna Group which is the basement of Viti Levu was the objective of the medium-wavelength anomaly analysis. Area of Yavuna Group distribution show marked high gravity anomaly for medium-wavelength, and its upper surface would be the most prominent density boundary at least in the northeast-northwest-western Viti Levu. The analysis was first made on the C - D profile where Yavuna Group is exposed, then A - B and E - F profiles were processed. The outcrop of Yavuna Group was selected as the control point for C - D profile, the calculated depth of the C - D at the profile intersection was used for A - B profile, and calculated depth of the A - B at the profile intersection was selected as the control point for E - F profile.

The results of the analysis with and the density contrast of 0.3 g/cm^3 and 0.5 g/cm^3 are shown, but the average depth of the density boundary from power spectral analysis is approximately 4.9 km, and the result with the density contrast of 0.3 g/cm^3 is more harmonious.

In short-wavelength anomaly analysis, there are localities with low density layers in the upper horizons and with low density layers in the lower horizons, and thus the densities were set by referring to geological maps.

For A - B profile, model with low density layers in the lower horizon was used because the high density Ba Volcanic Group and the Koroimavua Volcanic Group are widely distributed. Two results with $\Delta\rho$ = -0.2 g/cm^3 and -0.3 g/cm^3 are shown.

For C - D profile, model with low density layer ($\Delta\rho$ = -0.3 g/cm^3) in the lower horizon was used for the northern half because the Koroimavua Volcanic Group and the Ba Volcanic Group occur here, and model with low density layer ($\Delta\rho$ = 0.3 g/cm^3) in the upper horizon was used for the southern half because formations consisting mostly of sedimentary units (Tuva Group, Cuvu Group etc.) occur in this part.

For E - F profile, model with low density layer ($\Delta\rho$ =

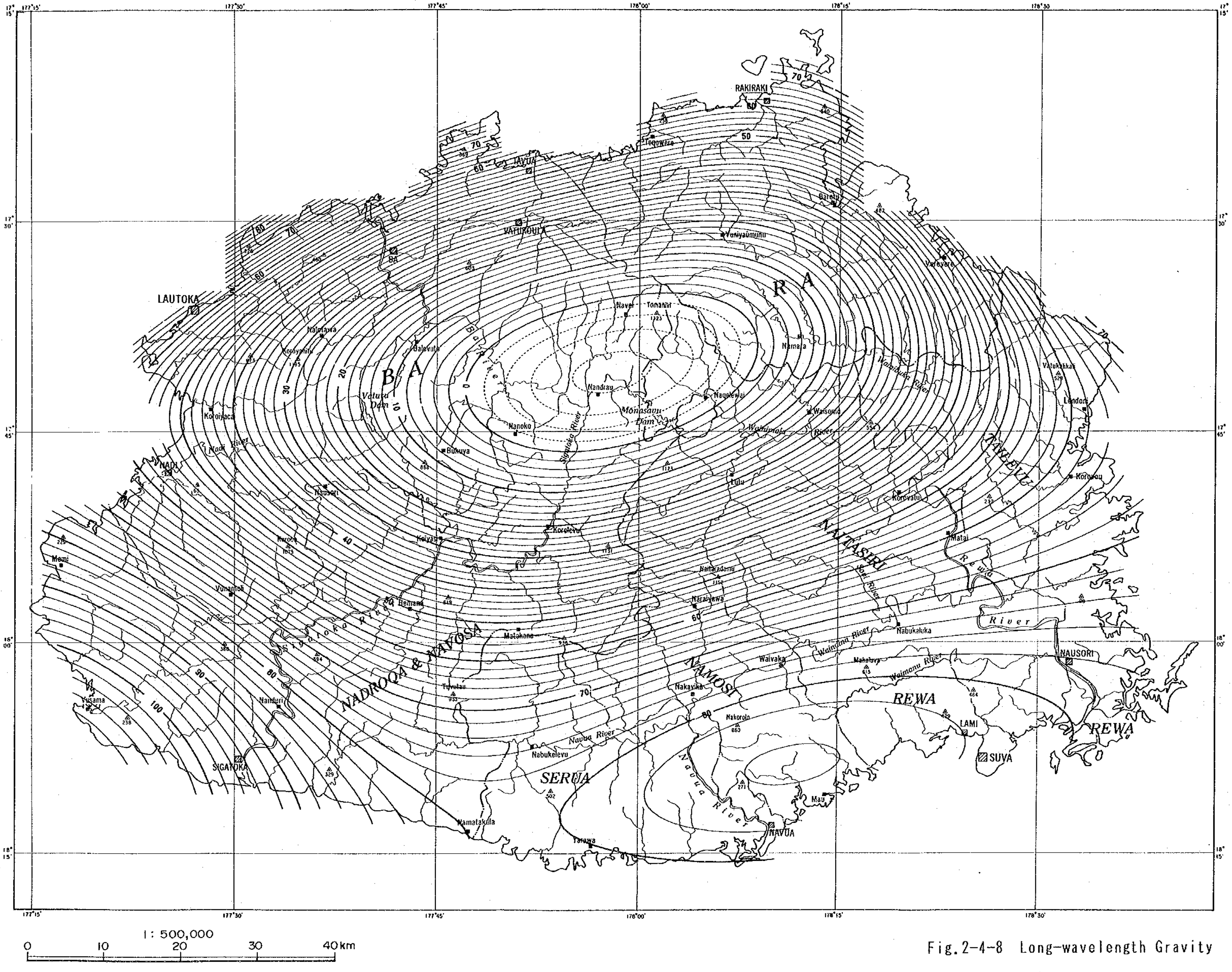

1 : 500,000

0 10 20 30 40km

LEGEND

Contour inteval : 2mgal

Fig.2-4-8 Long-wavelength Gravity

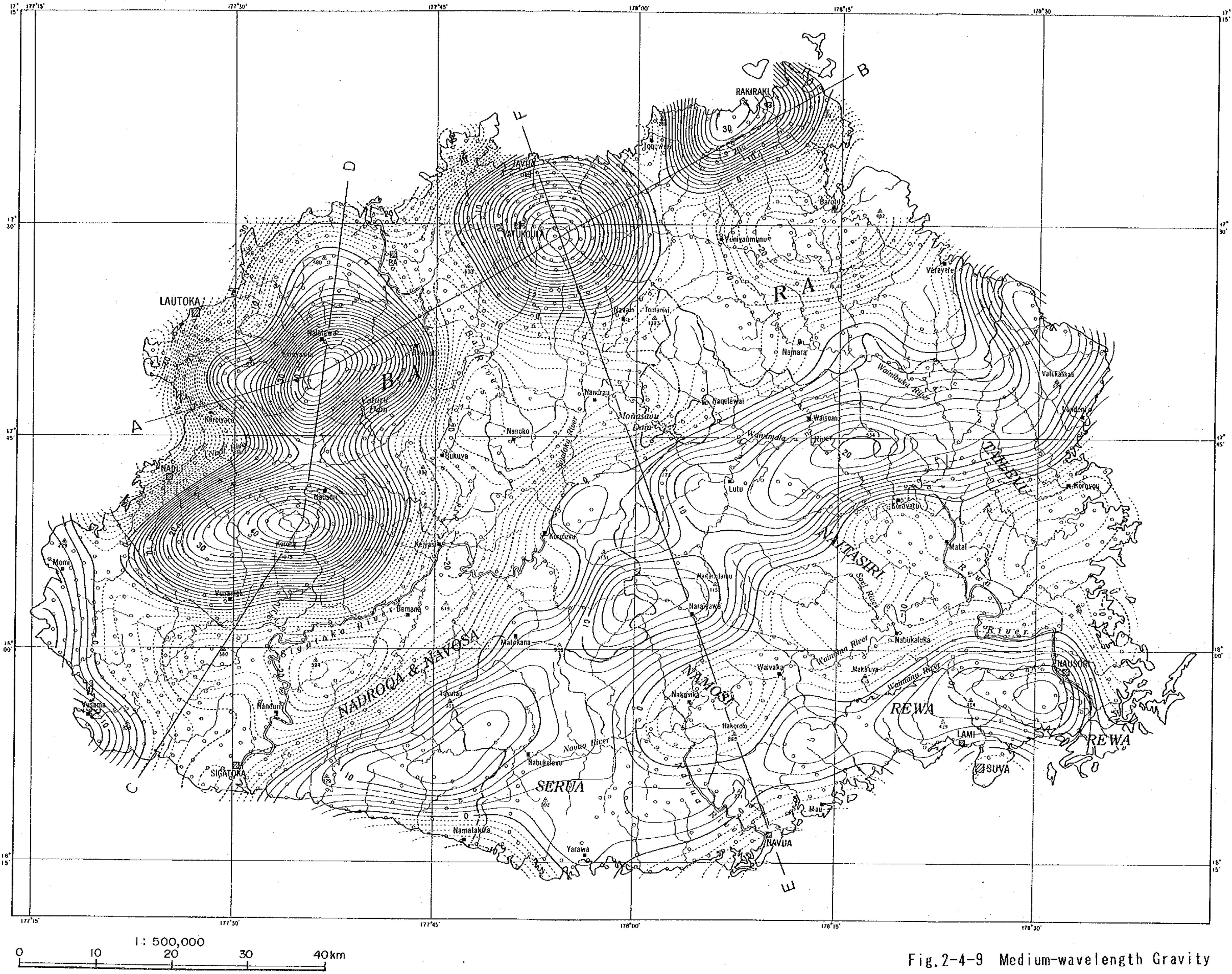

LEGEND

Contour inteval : 2mgal

A — B Section line

Fig.2-4-9 Medium-wavelength Gravity

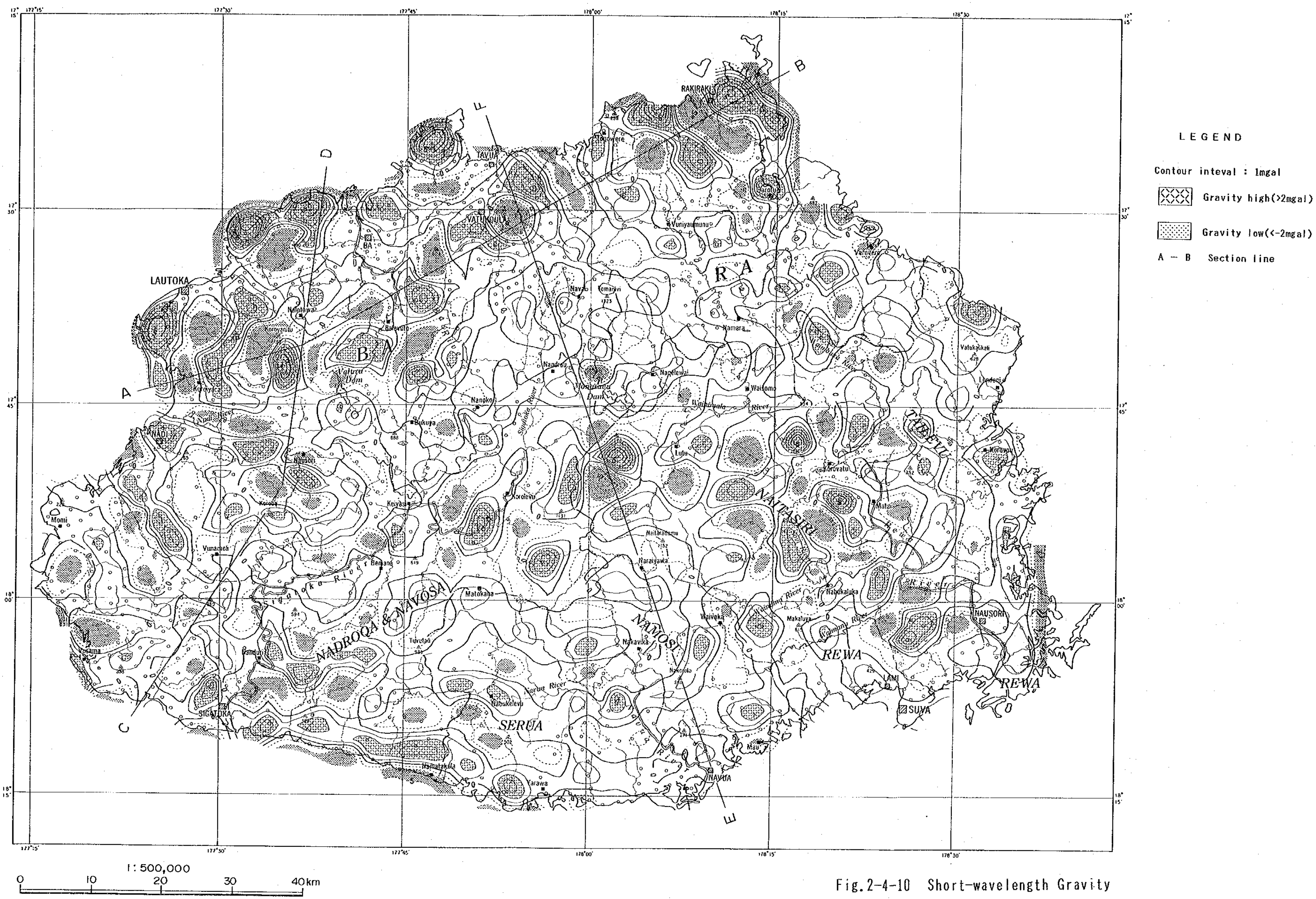

Fig.2-4-10 Short-wavelength Gravity

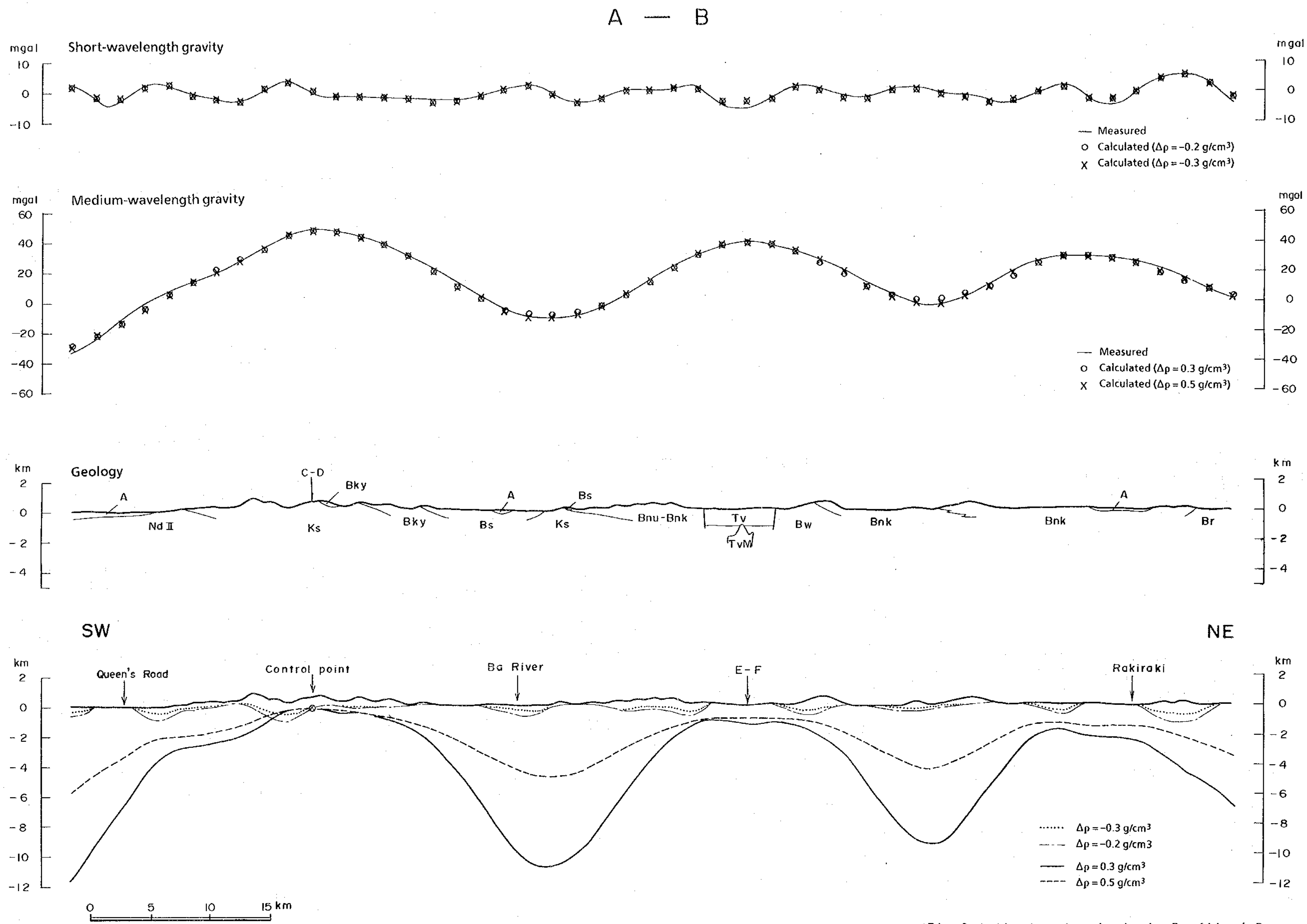

Fig.2-4-11 Gravity Analysis Profile A-B

LEGEND

ALLUVIAM
- A :Alluviam, beach sand, etc.

BA VOLVANIC GROUP
- TV :Tavua Volcanic Product
- Bnk :Nakorotubu Basalt
- Br :Rokavukavu Basalt
- Bnu :Nukunuku Lavas
- Bky :Koroyanitu Breccia
- TVM :Tavua Monzonite
- Bwn :Wainatio Volacanic Product
- Bka :Karavi Volcanics
- Bnm :Namosau Volcanics
- Bw :Wainivoce Trachybasalt
- Bmv :Muanisavu Sill
- Bs :Saru Shoshonite
- Bnd :Nadrou Creek Intrusives
- Bvk :Vatuknro Greywacke

CUVU SEDIMENTARY GROUP
- Cu :Sedimentary rocks

KOROIMAVUA VOLCANIC GROUP
- Ks :Sabeto Volcanics

NAVOSA SEDIMENTARY GROUP
- Nva :Andesitic Pyroclastic rocks

NADI SEDIMENTARY GROUP
- Nd II :Sandstone

MENDRAUSUCU GROUP
- Mnv :Navua Mudstone
- Mnm :Namosi Andesite

TUVA GROUP
- Tt :Takaro Congromerate
- Tc :Cici Sandstone

COLO PLUTONIC GROUP
- Ct :Tonalite, Diorite

WAINIMALA GROUP
- Wnm :Namalavu Congromerate
- Wtt :Tuvutau Greywacke
- Wnu :Nubuonaboto Volcanics
- Wta :Tari Formation
- Wla :Lawalevu Sandstone
- Wnd :Nadele Breccia
- Wnb :Nabu Formation
- Wm :Matawailevu Dacite

YAVUNA GROUP
- Yvs :Yavuna Stock(Tonalite)
- Yv :Yavuna volcanics

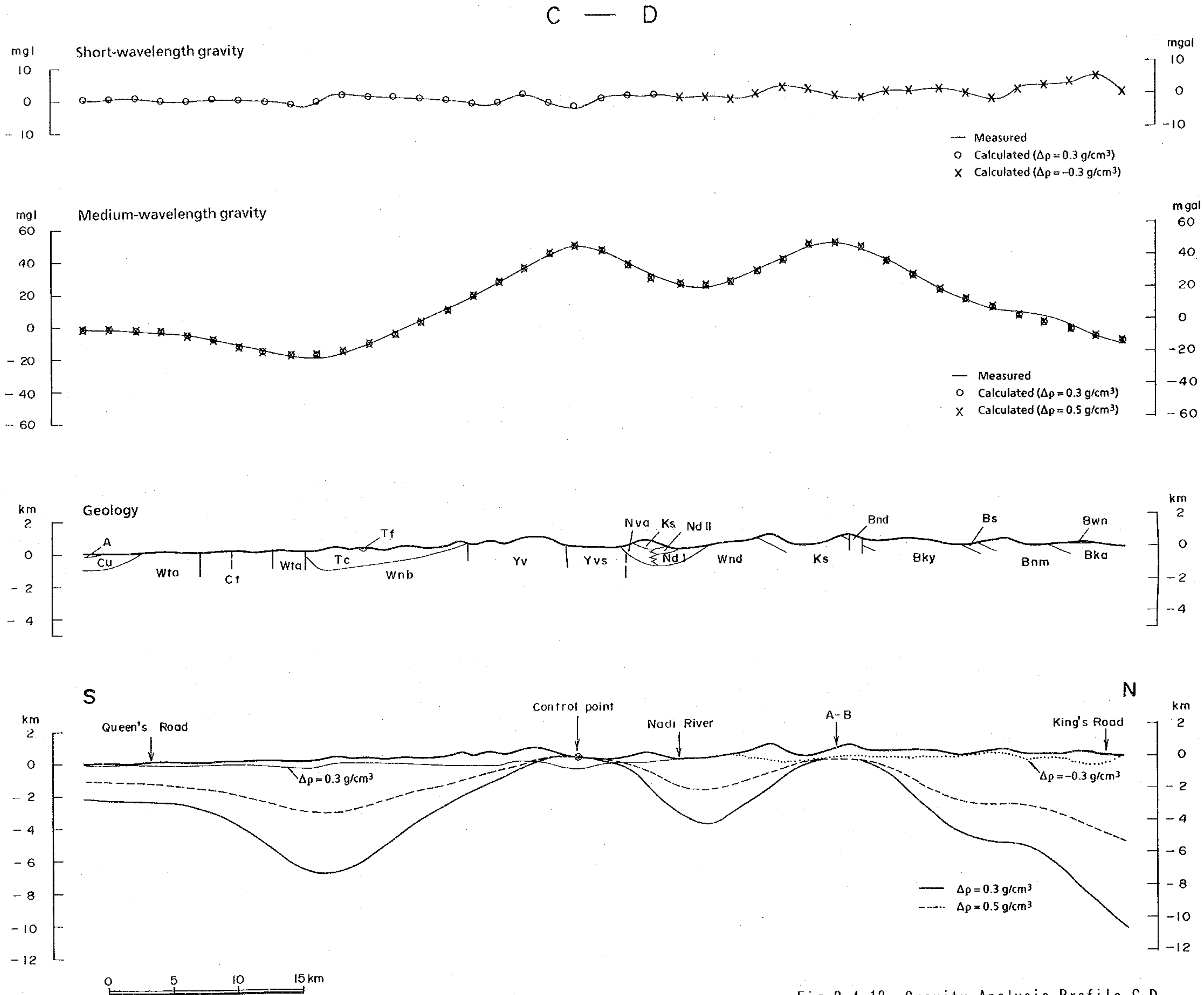

Fig. 2-4-12 Gravity Analysis Profile C-D

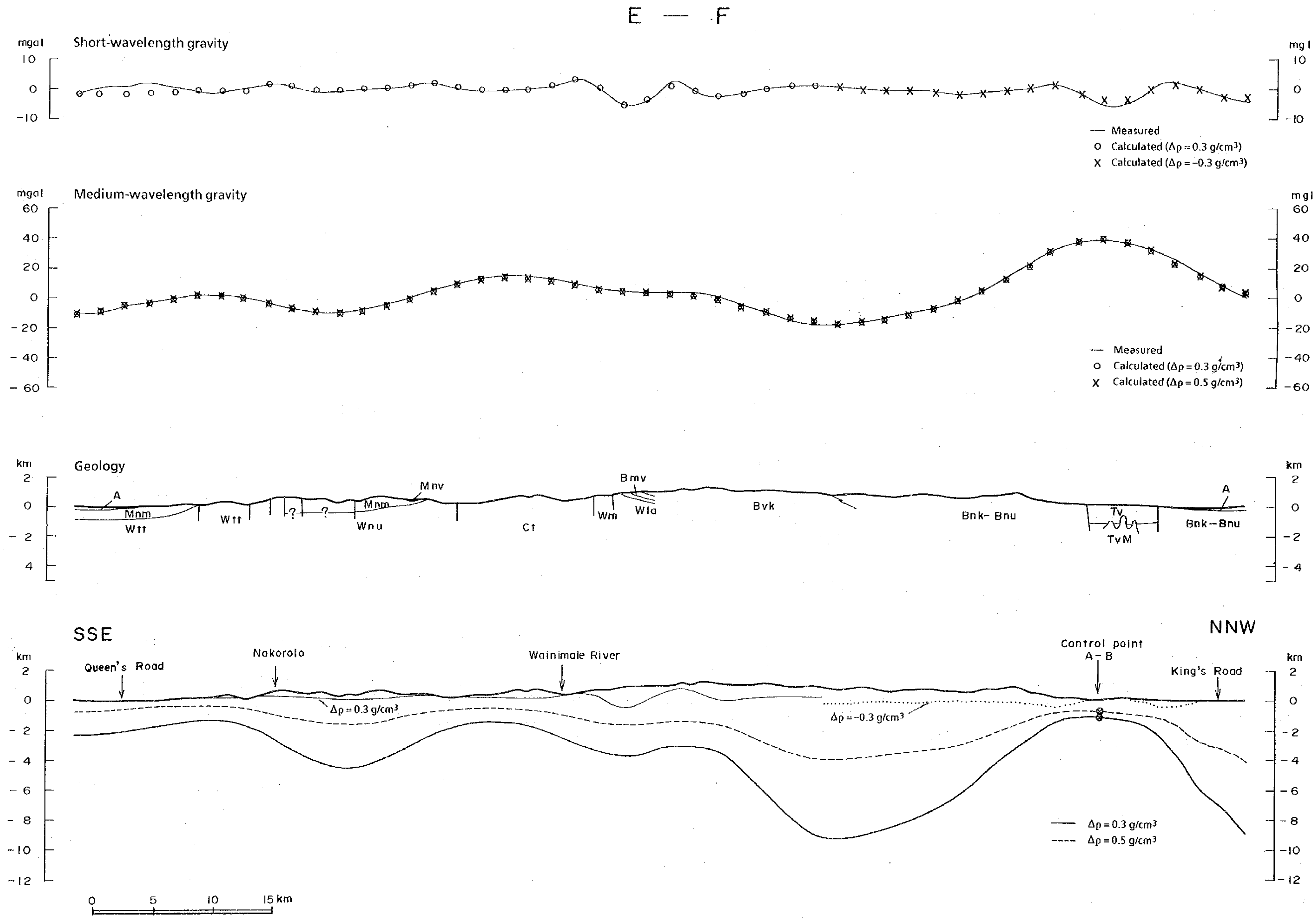

Fig. 2-4-13 Gravity Analysis Profile E-F

-0.3 g/cm³) in the lower horizon was used for the northern one third (1/3) because Ba Volcanics are distributed, and model with low density layers ($\Delta\rho$ = 0.3 g/cm³) in the upper horizon was used for the southern two thirds (2/3) because Medrausucu Group is distributed.

The depth of the basement (Yavuna Group) obtained by medium-wavelength high gravity anomalies with the assumption of $\Delta\rho$ = 0.3 g/cm³ is; about 1,000 m at the center of the medium-wavelength gravity high southwest of Ba, also about 1,000 m at the center of medium-wavelength gravity high east of Vatukoula, and 1,500 m at the center of high anomaly west of Rakiraki. The depth of the basement at the 'Sigatoka' area (C - D profile) in southwest Viti Levu and Namosi (E - F profile) in the southeast is 2,000 - 7,000m and 1,500 - 5,000 m respectively. the above figures are obtained under the assumption that the medium-wavelength anomalies are the reflection of the relief of the upper surface of the basement complex.

In reality, however, marked medium-wavelength high gravity is not only caused by the rise of the basement surface, but also by large high density igneous bodies resulting from the solidification of large scale magma. In the present case, when the high anomaly caused by the high density igneous body is subtracted, the variation of the gravity caused by the basement relief would be considerably smaller, and the depth would be shallower. But at present, data sufficient for estimating the contribution of the igneous bodies to the total gravity do not exist and it is difficult to estimate the changes in the calculated depth of the basement.

4 - 3 Discussions

4-3-1 Relation between gravity, geology and SLAR images in the prospective areas

During the first phase survey of the present project which was carried out in 1990, 15 areas, A - O , were extracted as promising for locating epi- to mesothermal mineralized zones (See Fig.2-4-14). These zones have been surveyed geologically. In the following sections, the geologic structure of these areas will be considered from gravity features. The geological maps, SLAR analysis maps, medium- to short-wavelength gravity maps are shown in Figures 2-4-15 to 21. In the following discussions, the parts enclosed in [ ] are the summary of the contents of the report of the first phase survey.

In the following discussions dome, caldera, and annular structures are all identified by SLAR, those identified by other means will be so mentioned.

(1) Area A (Fig. 2-4-15)

This zone is located in Tavua - Vatukoula in north Viti Levu and there is a circular depression called the Tavua Caldera. The Emperor Mine is located in the central part. The surface geology consists mostly of basalt lava/pyroclastics (Bnk, Bw) of the Ba Volcanic Group, and Tavua Volcanic Products (Tv) is distributed in the central part.

[An annular structure has been extracted in the central part of the area and a semi-caldera structure was identified to surround the former on the outside. There are a semi-annular and a semi-caldera structures to the east of the above annular structure and these are a size smaller than the former ones. To the northeast, there are similar structures even smaller which were extracted from aerial photographs.

The annular structure in the central part coincides with a circular surface depression. This depression is believed to be a volcanic collapsed structure because volcanic products (Tavua Volcanic Products) occurring within the depression are younger than those in the surrounding areas. It is also inferred that the collapsed structure was enlarged by erosion.

There are no direct evidences regarding the genesis of the smaller semi- annular and semi-caldera structures to the east. They could be structures related to intrusion.]

The medium-wavelength gravity map shows the existence of a large high gravity zone which covers most of the area with its center to the east of Vatukoula. Short-wavelength gravity map shows a notable circular gravity low with diameter of approximately 6.5 km to the east of Vatukoula, and notable gravity lows at two localities northeast and southwest of the above low anomaly.

The circular short-wavelength gravity low agrees very well with the annular structures and the distribution of the Tavua Volcanic Products. This low is the reflection of the Tavua Volcanic Products distributed in the annular structures. The Tavua Volcanic Products show marked low anomaly. This is harmonious with the fact that Tavua Volcanic Products is andesitic and the surrounding rocks are basaltic.

It is noted that the short-wavelength gravity low is located at the center of the medium-wavelength gravity high. The cause of the medium-wavelength high can be; ① rise of the basement, ② existence of large mass of high density rocks such as solidified magma chamber, ③ large scale uplift of the basement caused by magmatic intrusion. It appears that ② or ③ would be a reasonable inferrence from the large size of the gravity anomaly and the circular shape, and a coincidence with inffered volcanic center. Thus it is most probable that a large mass of high density rocks exist in the deeper parts.

The semi-caldera structure agrees with the contour of the medium-wavelength gravity high. This indicates relation of the structure with the gravity anomaly. No short-wavelength anomaly accompanies the small annular structures in the eastern part of the area.

The photogeological semi-annular and semi-caldera structures in the northeastern part of the area and the center of short-wavelength gravity high coincide. There are small bodies of diorite porphyrite and also dykes and faults are developed more or less in radial pattern in this semi-annular structure. From these facts, the report of the first phase pointed out the possibility of a structure with a intrusive body with cone-shaped top. The coincidence of the center of the short-wavelength gravity high and the semi-annular structure would support this hypothesis.

The short-wavelength gravity high in the southwestern part cannot be correlated to the type of structures discussed above. Blind high density intrusive bodies are inferred.

(2) Area B (Fig. 2-4-15)

This area lies adjacent to and east of Area A. The surface geology consists of basalt lava and basaltic pyroclastics (Bnk) of the Ba Volcanic Group.

[Semi-annular and semi-caldera structures have been extracted in this area, but direct evidences relating them to be collapsed structure have not been found by geological survey.]

This area is on the eastern side of the marked medium-wavelength gravity high discussed in the preceding Area A. It is also on the SSE extension of the short-wavelength low gravity zone (below -2 mgal) shown elongated in the NNW-SSE direction in the short-wavelength gravity map. Notable gravity anomalies are not found to be associated with the SLAR structures. This indicates that these SLAR structures do not involve density contrast of any significance, but it is also a fact that the gravity measurements of these structures are sparse and the gravity features is not sufficiently understood.

(3) Area C (Fig. 2-4-16)

This is located at the northeastern edge of Viti Levu. The surface geology consists mostly of basalt lava and basaltic pyroclastics (Bnk) of the Ba Volcanic Group.

[Annular, semi-caldera, and dome structures have been extracted in this area. It is considered that the dome is a volcanic dome formed in relation to the intrusion of magma. The supporting evidences for this are; semi-dome type geologic structure in the vicinity, occurrence of gabbro (Bns) in the central part of the dome, andesite plugs in the vicinity, and radial arrangement of dykes.]

This area, according to the medium-wavelength gravity map, is located at the large scale oval-shaped gravity high with the center to the west of Rakiraki. The short-wavelength gravity map shows that NW-SE trending belt-form anomaly zones are arranged from the east westward; high, low, high. This zonal arrangement gravity anomalies becomes vague further west, but the pattern continues on.

The dome structure coincides with the marked short-wavelength gravity high. The northeastern semi-annular and the east-southeastern semi-caldera structures coincide with the marked short-wavelength gravity low. The short-wavelength gravity features is characteristically distributed in the NW-SE direction while the SLAR structures do not have this trend. The marked short-wavelength gravity high which coincides with the dome probably reflect the high density gabbro (Bns) which occur at the dome.

The semi-annular structure to the northeast of the dome and the semi-caldera structure to the east-southeast of the dome coincide with marked short-wavelength gravity low. Basaltic rocks with relatively high density are the predominant geologic unit of this area (Bnk), and the low gravity is interpreted to represent the dominance of low density pyroclastics in the area or thick occurrence of low density sedimentary rocks (Buk, Bvk) under the basaltic unit.

Regarding the SLAR structures in the southwest, and the semi-caldera structures continuing from the east to the southwest, corresponding short-wavelength gravity anomalies have not been found. With medium-wavelength gravity anomalies, however, the dome and the semi-annular structures are in the center of the high anomaly and the semi-caldera opening north to northwestward is in harmony with the gravity contours. This indicates the existence of some relation between the deeper structure and that shown in the SLAR images.

The short-wavelength gravity high to the southeast of the dome and the short-wavelength gravity high east of Rakiraki probably reflects the blind intrusive bodies such as gabbro.

The medium-wavelength gravity high of this area suggests the possibility of large mass of high density rocks in the deeper parts as in the case of Area A.

(4) Area D (Fig. 2-4-16)

This area is located to the southeast of Area C. The surface geology mostly consists of sandstone and conglomerate (Rb, Rw) of Ra Sedimentary Group, and greywacke and sandstone (Bvk), basalt lava and pyroclastics (Br, Gnk)of Ba Volcanic Group.

[Dome structures have been extracted in four localities of this area, and semi-caldera structures extracted from the east to the southern border. The domes in this area are considered to be of volcanic nature from the existence of craters at the top and intrusion of micro diorite in the sandstone to the northeast.]

The medium-wavelength gravity map shows this area to be a low gravity area below -10 mgal. Regarding the short-wavelength gravity features, there is a relatively high anomaly near Barotu in the north, but otherwise anomalies are weak, the low is within -3 mgal.

There are domes in two localities in the east, the eastern one coincides with the short-wavelength gravity low southeast of Barotu, and the western one almost coincides with the short-wavelength gravity high near Barotu. The short-wavelength gravity low southeast of Barotu is located at the inferred volcanic center. The short-wavelength gravity high near Barotu could possibly be due to blind intrusive bodies within sedimentary formations because high density rocks do not occur on the surface.

There are also domes in two localities in the west, corresponding short-wavelength anomalies have not been confirmed. Same applies for semi-caldera in this part. The area where domes occur, medium-wavelength gravity low are usually developed and low density Ra Sedimentary Group is expected to be thickly deposited. Under such environment, it is believed that intrusive bodies in shallow zones would result in marked short-wavelength gravity high as in the case of near Barotu.